Comparative Medicine
Copyright 2015
by the American Association for Laboratory Animal Science

Vol 65, No 2
April 2015
Pages 96–113

Overview

Practical Murine Hematopathology: A Comparative Review and Implications for Research

Karyn E O'Connell,[1] Amy M Mikkola,[2] Aaron M Stepanek,[2,11] Andyna Vernet,[2,10] Christopher D Hall,[2] Chia C Sun,[3,4,12] Eda Yildirim,[5,13] John F Staropoli,[6,7,14] Jeannie T Lee,[5,7–9] and Diane E Brown[2,*7]

Hematologic parameters are important markers of disease in human and veterinary medicine. Biomedical research has benefited from mouse models that recapitulate such disease, thus expanding knowledge of pathogenetic mechanisms and investigative therapies that translate across species. Mice in health have many notable hematologic differences from humans and other veterinary species, including smaller erythrocytes, higher percentage of circulating reticulocytes or polychromasia, lower peripheral blood neutrophil and higher peripheral blood and bone marrow lymphocyte percentages, variable leukocyte morphologies, physiologic splenic hematopoiesis and iron storage, and more numerous and shorter-lived erythrocytes and platelets. For accurate and complete hematologic analyses of disease and response to investigative therapeutic interventions, these differences and the unique features of murine hematopathology must be understood. Here we review murine hematology and hematopathology for practical application to translational investigation.

Abbreviations: GEM, genetically engineered mouse; NMB, new methylene blue; nRBC, nucleated RBC; RDW, RBC distribution width; TNCC, total nucleated cell count.

Hematology is an important adjunct to both clinical medicine and biomedical research, with more than 1700 currently funded NIH projects[109] and more than 3400 research articles published over the past 5 years using mouse models.[120] There are now more than 6000 genetically engineered mouse (GEM) models of disease, with 500 new GEM created each year at the Jackson Laboratory alone, and several large projects are underway to thoroughly phenotype each new mutant mouse strain (https://www.komp.org/).[13,176] A mouse tumor database (http://tumor.informatics.jax.org/mtbwi/index.do) is available to provide information regarding mouse models of human cancer, and the Mouse Phenome Database at the Jackson Laboratory provides links to phenotypic data for many GEM models (http://phenome.jax.org/).[8] The defined components to complete the phenotyping of GEM models have been recently reviewed.[13,157,176] In addition, 21 inbred strains of mice are commonly used for investigations into such topics as response to infectious and genetically induced disease and dietary and pharmacologic therapies. These commonly used laboratory mouse strains have, for example, inherent differences in immunology or iron trafficking, which can affect research outcomes.[16,47,137] These interstrain differences are important to recognize and understand as a component of effective study design and prior to strain selection for laboratory investigations, especially when hematologic responses to disease need to be considered.[13,16,137]

For any appropriately designed experiment, concurrent age-, sex-, and strain-matched control mice must be included to accurately compare the effects of a disease, genetic manipulation or therapeutic intervention;[13,155] alternatively, individual mice can be used as their own controls in some studies. Several important guidelines exist to ensure that appropriate numbers of experimental and control mice are incorporated into a study design to maximize statistical power yet minimize waste.[13,40-42,71,72,176] During and between studies, consistent blood collection methods are essential for accurate comparative analyses. Species-appropriate hematologic instrumentation and timely analysis of fresh blood are necessary to minimize preanalytic hematologic errors.[3,37,71] Especially important for mice and their restricted available blood volume are the use of practical, accurate, species-specific, and up-to-date hematologic methods.

Here we comprehensively review murine hematology and hematopathologic responses to disease in the context of biomedical research, discovery, and phenotyping studies. To maximize the opportunity for detecting phenotypes, disease, and responses to therapeutic interventions in mice, we focus on providing a practical summary of methods and analysis for accurate hematologic

Received: 16 Oct 2014. Revision requested: 09 Nov 2014. Accepted: 25 Dec 2014.
[1]Department of Comparative Pathology, New England Primate Research Center, Harvard Medical School, Southboro, Massachusetts; [2]Center for Comparative Medicine, [3]Program in Anemia Signaling Research, Nephrology Division, [4]Program in Membrane Biology, Center for Systems Biology, [5]Department of Molecular Biology, and [6]Molecular Neurogenetics Unit, Center for Human Genetic Research, Massachusetts General Hospital, Boston, Massachusetts; [7]Department of Pathology and [8]Howard Hughes Medical Institute, Harvard Medical School, Massachusetts General Hospital, Boston, Massachusetts; [9]Department of Genetics, Harvard Medical School, Boston, Massachusetts. Current affiliations: [10]Wyss Institute for Biologically Inspired Engineering, Harvard Medical School, Boston, Massachusetts; [11]Public Health and Professional Degree Program, Tufts University School of Medicine, Boston, Massachusetts; [12]Cellular and Translational Immunology, EMD Serono Research and Development Institute, Billerica, Massachusetts; [13]Department of Cell Biology, Duke University Medical Center, Durham, North Carolina; and [14]Biogen Idec, Cambridge, Massachusetts.
** Corresponding author. Email: dbrown31@mgh.harvard.edu*

studies and on describing the morphologic assessment of mouse hematopathology in peripheral blood and bone marrow in ways that will be useful to those—veterinarians and researchers alike—who work with murine species.

Murine Hematology: General Considerations

Minimizing preanalytic variables. Several factors impact the ability to obtain meaningful hematologic results from blood samples in mice with limited available blood volume. Frequency of blood collection, size and age of the mice, and available hematologic instrumentation all play a role in blood volume limitations and ultimately in the quality of the data generated. In particular, variability in fasting or anesthetic protocols or blood collection site can affect results.[142,155] For example, fasting protocols not standardized between studies may introduce preanalytic variation because mice consume less water while fasting than otherwise, potentially resulting in hemoconcentration[36] and causing an artifactual increase in Hct. Preanalytic factors to consider include sex, strain, age, altitude, and vendor[116] and environmental variables such as diet, housing, and SPF status of the mouse colony.[13] A factor specific to hematologic analyses is the propensity for mouse platelets to clump.[105,176] Therefore, the use of a consistent collection site and method, handling that minimizes stress and allows for the collection of a sufficient volume of blood, and appropriate anticoagulation are imperative to minimizing preanalytic variables and thus ensuring accurate hematologic analysis and interpretation.

Features of peripheral blood. Mice have small erythrocytes (RBC), compared with other mammalian species, and the lifespans of erythrocytes and platelets in mice are generally shorter than those in humans and other veterinary species. Consequently mice maintain a somewhat regenerative state, normally having between 1% to 6% circulating reticulocytes, resulting in polychromasia and slight anisocytosis on Wright–Giemsa-stained blood films.[37,130] 'Ringform' nuclear morphology, characterized by a circular nucleus, is a normal feature of mouse neutrophils, eosinophils, and monocytes.[10] Mice have very high platelet counts (9 to $16 \times 10^5/\mu L$) compared with those of other mammals,[37,100,105,119] a contributing factor to the aforementioned potential for platelet clumping.

Features of bone marrow. A complete assessment of hematologic status in mice should include evaluation of bone marrow and spleen in addition to peripheral blood. Preparation of bone marrow samples for cytology in mice is best accomplished by using the 'paintbrush technique' (see Methods), which preserves cellular morphology and evenly distributes cells on glass slides.[37] Bone marrow cellularity is higher for mice than other species and does not decrease with age, as it does in humans, but the proliferative capacity of murine hematopoietic stem cells is decreased.[37,100,130] Both granulocytic and monocytic precursors can have ring-shaped nuclei.

Features of the spleen. In mice, the spleen is the primary site for body iron storage[114,153] and remains an active site for hematopoiesis throughout life. The potential for exuberant extramedullary hematopoiesis in response to anemia must be recognized in this species.[16,17,156] Therefore, the role of the spleen should be considered in any evaluation of hematopoiesis, and this organ should be evaluated in addition to the bone marrow to fully characterize a hematologic phenotype or response to therapy.[47,127]

Methods for Collecting High-Quality Blood Samples and for Accurate Hematologic Analyses

Study Design. The sample size for any experimental design ultimately depends on the variability of the outcomes; for hematology, variability can be established by using appropriate control groups. Pilot studies can be helpful for predicting variability. A statistician should participate in the determination of sample size by power analysis to ensure that hematologic data meet test assumptions and to account for experimental error[176](http://www.uml.edu/Research/OIC/animal-use/helpful-links.aspx). Experimental design for animal studies has been reviewed elsewhere.[41,42,71,72,131,155] The goal should always be minimizing use of animals while allowing for sufficient power to determine the effects of an intervention.

Blood collection. *Volume.* The average reported blood volume in mice is 7.8 mL per 100 g of body weight.[37,90] Therefore the total blood volume in 9- to 10-wk-old mice is approximately 2 mL, making the maximal volume that can be collected safely at a single survival time point approximately 200 µL. Previous studies in rodents indicate that although serial blood sampling is possible, it requires a postphlebotomy recovery period that depends on the withdrawn volume;[20,37] the maximal collection of 15% blood volume with a 4-wk recovery period has been recommended for mice.[37,90] More frequent or greater blood volume collection than this recommendation has been reported, with recovery defined as the return of mean Hgb values to within 2 SD of mean baseline values provided that no weight loss, behavioral changes, or clinically significant anemia has occurred.[123] However, adhering to these alternative criteria may lead to important changes in the hemogram that could alter study outcomes.

Collection site. The method and site of blood collection in rodents can influence results.[87,100] The submandibular venipuncture blood collection method is recognized to obviate the need for anesthesia, thus removing that potentially confounding variable while minimizing animal distress.[39,48] When performed by trained personnel and with immediate and appropriate mixing of anticoagulated blood samples, we have found that blood collection by submandibular venipuncture can significantly reduce platelet clumping. Although excessive bleeding after submandibular collection in mice with abnormal coagulation is reported,[61] this complication can occur at any collection site in these models, which may therefore require prolonged compression and monitoring after blood collection. Scientific studies frequently report platelet clumping as an issue when collecting blood from mice; therefore some authors subsequently either do not report platelet counts or report artifactually low counts when clumping is suspected.[94,105] Because platelet clumps lead to decreased automated platelet counts, such data always warrant review of a blood film[84,90] to verify thrombocytopenia. Another site historically included for survival blood collection is the retroorbital sinus, but this site is no longer recommended in light of tissue trauma, contaminated and clumped samples, postcollection morbidity, and the need for anesthesia.[37,59,87,155] For terminal samples, cardiocentesis can be performed in sufficiently anesthetized mice and, when performed quickly and efficiently, enables the collection of large sample volumes without platelet clumping. Care must be taken during cardiocentesis to avoid puncturing other viscera and potential contamination of the sample with nonblood cells. Other perimortem collection sites include the aorta and caudal vena cava.[37]

Sample handling. Blood samples can be collected directly into an anticoagulant, such as EDTA. Because EDTA (K_2 or K_3) causes less postcollection platelet clumping and provides better staining characteristics, it is preferred over heparin as an anticoagulant for rodent blood.[37,51,82,155] In addition, EDTA is the preferred anticoagulant for most automated analyzers. For greatest accuracy, blood films should be prepared (Figure 1 A) and samples analyzed by automated methods within 4 h and not longer than 24 h after collection. One study using an automated analyzer found increased MCV, RBC distribution width (RDW), and MPV and decreased MCHC and monocyte counts in CD1 mice after storage of blood for 24 h at 4 °C.[3] Blood collection tubes should be filled to recommended volume to ensure the correct blood:anticoagulant ratio, and blood should be mixed by inversion gently and immediately after collection to ensure adequate distribution of the anticoagulant. To avoid artifactual hemolysis of samples (Figure 1 B), the blood tube should not be shaken, and the needle should be removed from the syringe prior to dispensing blood into the collection tube to avoid shearing of cells. Although mouse blood samples can be diluted for automated analyzers that require large sample volumes, the accuracy and precision of diluted samples are highly variable,[37] and modern automated veterinary analyzers require relatively small sample volumes for CBC analysis (for example, 20 µL [Heska HemaTrue], 50 µL [Idexx ProCyte]), making survival and sequential sampling designs feasible.

Slide preparation. Fresh blood films should be prepared at room temperature and stained within 4 h of collection by using anticoagulated blood that is well-mixed. Mixing is important and can be performed manually by gently inverting the tube 5 to 10 times or by placing on a tilting or rotating rack designed for mixing blood. A clean microhematocrit tube or pipette then is used to dispense a drop of blood onto one end of a clean microscope slide. A second slide is placed at an angle of 30° to 45° in front of the drop of blood and then is backed into the drop of blood. Once the blood droplet has spread along the edge of the angled slide, it is then pushed forward in a single rapid motion to create the classic 'half-moon' profile that provides a monolayer for cell counting (Figure 1 A).[168] To avoid cellular morphology artifacts, the blood film must be allowed to air dry fully (typically at least 30 to 45 min, depending on humidity and temperature) before being stained with a Romanowsky-type stain for review (Figure 1 C).[62,168] Unfixed slides can be saved for future use (for example, additional stains, confirmation of results).

Manual WBC counts and correction for nucleated RBC (nRBC). A manual leukocyte differential count is important for hematologic analyses in all species, and mice in particular, given that available veterinary analyzers have not yet been validated fully for use in mice;[94,158] in this analysis, 100 (or 200 to 500, for improved accuracy) WBC are counted and categorized.[62] Cell-type percentages then are multiplied by the total WBC count (generally obtained from an automated analyzer) to determine the absolute count for each cell type. To correct the WBC count when nRBC comprise greater than 5% of the total nucleated cell count (TNCC), the number of nRBC per 100 nucleated cells is determined through blood-film review, and the TNCC (or total WBC count), typically from an automated analyzer, is multiplied by 100 / (no. of nRBC + 100).[148]

Ancillary tests. At the time of slide preparation, it is also useful to perform a PCV or spun Hct measurement. A small aliquot of blood is drawn into a capillary tube and sealed with tube sealant on one end. The tube then is spun in a microhematocrit centrifuge for more than 3 min, separating the blood components into 3 layers—plasma, buffy coat (WBC), and packed erythrocytes. Icterus, lipemia, and hemolysis can be detected by holding the capillary tube against a white background. The total protein concentration can be estimated by breaking the tube and loading the plasma into a refractometer. Reticulocyte counts can be obtained from some automated analyzers (ProCyte, Advia), if validated, or can be performed manually. For manual reticulocyte enumeration, whole anticoagulated blood is mixed with new methylene blue (NMB) and allowed to incubate for 10 to 20 min, after which a blood film is made (Figure 1 D).[62] An absolute reticulocyte count is achieved by multiplying the percentage of reticulocytes (usually determined by counting the number of reticulocytes per 500 to 1000 RBC) by the absolute RBC count.[28]

Reference Intervals

Historical reference intervals are available in textbooks,[66,100,119] journal articles[94,105,116] and on the Internet (Jackson Laboratory's Mouse Phenome Database, Knockout Mouse Project, https://www.komp.org/). However, because of variability due to laboratory instrumentation, methods, collection sites, strain, age, sex, and environmental factors, reference intervals are best generated inhouse for any specific experimental population.[105,155] Individual mice in study groups can be compared with their own baselines, or group comparisons can be made.[127] In addition, individual reference intervals are starting to gain popularity[162] and can be an option for mice now that serial, survival CBC counts are practical given the availability of microvolume, automated analyzers. Reference intervals should be used as a tool, not as the sole guide to determine normalcy.[119] In our experience, the single best way to detect an important hematologic phenotype, effect of disease, or response to therapy is to generate concurrent age-, strain-, and sex-matched controls for experiments, by using consistent sample collection and analysis methodologies including collection time, site, fasting status, and automated analyzer.

Peripheral Blood: General Considerations and Responses to Disease

Erythrocytes in health and disease. Murine RBC are spherical, anucleate biconcave discs with central pallor (Figure 1 C) that are approximately 4 to 7 µm in diameter. In general, total RBC counts range from 7800 to 10,600 per microliter.[87,119] However, because counts vary with mouse strain, automated analyzer, and other factors, experiment-specific age-, strain-, and sex-matched controls should always be included to detect important experimental differences. Hct, which is a measure of RBC volume, is lower in very young and very old mice because of their lower RBC absolute count and expanded plasma volume, respectively.[37,130] In healthy control mice, Hct ranges from 35% to 52%, and in general, should be 3 times the Hgb concentration.[37,100,130,166,168] Importantly, when automated analyzers use spectral analysis, hemolysis can alter MCV and therefore the calculated Hct value. A spun PCV analysis, which is essentially a manual Hct determination, can be performed to confirm an automated Hct value and should be used when there is a mismatch of the 3:1 Hct:Hgb ratio. Mice have small RBC compared with that of most other mammalian species, with an average MCV of 45 to 55 fL in health. The normal

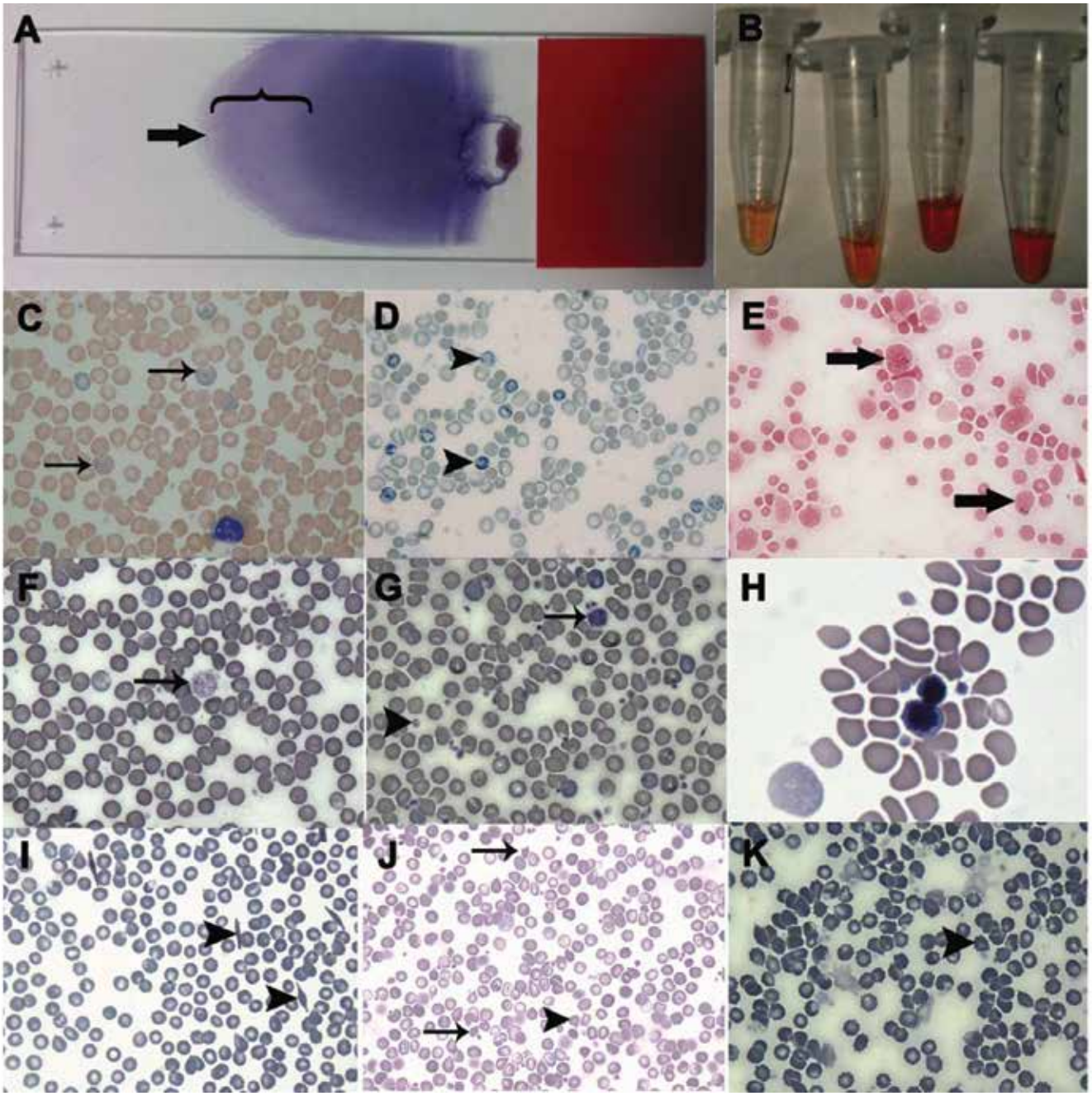

Figure 1. Features of mouse peripheral blood: RBC and platelet morphologies. (A) Example of a blood film stained with a Romanowsky type stain showing the classic 'half-moon' appearance and feathered edge (arrow); bracket highlights the monolayer counting area. (B) Examples of hemolyzed plasma, which is due to poor collection method or disease and can interfere with automated hematologic analyses. (C) Normal erythrocytes and platelets with a normal percentage (approximately 1% in this case) of polychromatophilic erythrocytes (arrows). (D) New methylene blue staining showing remnant RNA in reticulocytes (arrowhead). (E) Prussian blue staining showing atypical iron inclusions in an erythroid precursor (top arrow) and erythrocyte (bottom arrow). (F) A megaplatelet (arrow) is markedly larger than surrounding erythrocytes. (G) Giant platelets (arrow) are approximately the same size as erythrocytes, compared with the much smaller, normal platelets (arrowhead). (H) Circulating atypical nucleated erythrocyte (nRBC) undergoing nuclear division. (I) Sickled RBC (arrowheads) induced by a genetic mutation. (J) Iron deficiency induced by a genetic mutation (*tmprss6*$^{-/-}$) has led to anisocytosis, fragmented (thin arrows) and microcytic RBC (arrowhead). (K) Echinocytes (spiculated RBC, arrowhead) in a mouse model of polycystic kidney disease (CD1$^{pcy/pcy}$) with anemia and renal failure. Wright–Giemsa staining except where noted; original magnification, ×100.

mouse MCHC usually is 30 to 38 g/dL; the RDW, which reflects variation in RBC size, can fluctuate greatly depending on instrumentation[119] and the number of circulating larger immature (polychromatophilic) RBC, even in healthy mice.

Anisocytosis (that is, variation in RBC size) is a common feature seen on Wright–Giemsa-stained blood films because of the normal presence of polychromatophilic cells, which are larger than mature RBC, and is reflected in the RDW value. Mouse RBC

have a halflife of 38 to 52 d, which is shorter than that in humans and other veterinary species.[37,100,130] Polychromasia is identified on Wright–Giemsa-stained blood films as increased cytoplasmic basophilia due to increased RNA content. Polychromatophilic erythrocytes are anucleate and generally larger relative to the orange-red mature RBC (Figure 1 C), and when increased in number, indicate an erythropoietic response to anemia. Reticulocytes are polychromatophilic erythrocytes that are identified and manually counted by using NMB-stained preparations, in which RNA networks are visible as aggregates of dark-blue stain (Figure 1 D). Alternatively reticulocytes can be counted by using automated analyzers with murine-validated reticulocyte enumeration capability. Reticulocyte counts are reported as a percentage of the total RBC count or as an absolute number, with absolute numbers generally preferred for the interpretation of a regenerative response.[28,119] In addition, low numbers of nucleated RBC precursors or metarubricytes (<5%) can occur in peripheral blood films of healthy mice and increase during both physiologic and pathologic erythroid regenerative responses.[100,174] Correction of the WBC count is recommended when nucleated RBC (nRBC) are greater than 5% of the TNCC (see Methods section). In addition, Howell–Jolly bodies (micronuclei) can occur in mouse RBC (Figure 2 H).[37,100] The number of nRBC or Howell–Jolly bodies (or both) may increase in response to diseases causing anemia, inadequate splenic function, or myelodysplastic syndrome and myeloproliferative disorders.[37,64,101,121,125,133,174] Heinz bodies, which are cellular inclusions of denatured hemoglobin, result from oxidative injury, such as occurs after phenylhydrazine administration.[23]

Abnormalities in total RBC numbers or cellular morphology can be detected on review of Wright–Giemsa-stained blood films. Decreased RBC counts (anemia) occur secondary to conditions that include blood loss, immune-mediated hemolysis, inflammatory disease, renal disease, iron deficiency, myelodysplastic disease, genetic disorders, and neoplasia.[16,17,26,74,89,147,152,174] CD47 is important to the recognition of RBC by phagocytes, because the absence of this protein leads to severe immune-mediated hemolytic anemia.[110] Mice with exuberant regenerative responses to anemia can have increased anisocytosis (increased RDW) or macrocytosis (increased MCV) and low numbers of circulating early erythroid precursors, such as rubriblasts, prorubricytes, and metarubricytes, which are all nucleated forms of RBC. Importantly, GEM models of disease and disease states such as myelodysplasia and neoplasia can present with erythroid dysplastic changes including increased numbers of circulating megaloblastic rubricytes, sideroblasts, and siderocytes (identified by using Prussian blue staining; Figure 1 E), normochromic macrocytes and other nuclear:cytoplasmic asynchrony, and nuclear changes including multiple (Figure 1 H), fragmented, or lobulated nuclei; atypical mitoses; abnormal chromatin patterns; and prominent nucleoli.[11,125,147,159,174] An increased RBC count (polycythemia) may be relative or absolute. Relative polycythemia is caused by hemoconcentration secondary to dehydration, high altitude, myelodysplasia, or neoplasia.[37] Absolute polycythemia may be caused by increased erythropoietin production in response to anemia or hypoxia or by genetic mutations, such as overexpression of the Kit protein, that cause increased erythropoiesis.[15,32,130]

Poikilocytosis (variation in RBC shape) can take many forms, including acanthocytes, dacryocytes, eccentrocytes, echinocytes, keratocytes, schistocytes, spherocytes, stomatocytes, and target cells (Figure 1 I, K). RBC morphology can provide clues to pathogenesis in many diseases, and characteristics identified by a simple blood film review can aid tremendously in the interpretation of disease model phenotypes. Some examples of disease and their characteristic RBC morphologies include iron deficiency (schistocytes, microcytes, keratocytes; Figure 1J), liver disease (target cells, acanthocytes), disseminated intravascular coagulation (schistocytes), immune-mediated hemolytic anemia (spherocytes), renal disease (echinocytes; Figure 1K), and myelofibrosis (dacryocytes).

Leukocytes in health and disease. The typical WBC count in mice is 2000 to 10,000 per microliter.[100,119] In general, an automated total WBC count is more precise and accurate than is a manual count, because many more cells are counted during automated analysis. However, reviewing the blood film is an important quality-control check, especially when results are beyond the normal range, to confirm TNCC and automated WBC differential counts, define severe leukopenia or leukocytosis, determine left shifts (increased number of immature granulocytes in peripheral blood), and identify cells with atypical morphology (Figure 2 E, G). A quick scan of the feathered edge (Figure 1 A) is an important component of any slide review and serves to identify large atypical cells, platelet clumps, mast cells, nonhematopoietic cells, and parasites.[168] Many disease phenotypes can be better characterized and diagnosed after careful review of a stained blood film. Automated analyzers tend to undercount mouse monocytes, for example, and often will not differentiate atypical lymphocytes, granulocyte types (Figure 2 A, B), bands and early myeloid precursors, nRBC, or neoplastic cells.[4,7,17,53,,113,145] Differentiating types of leukocytes can pose a challenge in mice due to their unique morphologic characteristics including, for example, the ring forms normally seen in both granulocytic and monocytic lineages (Figure 2 C, D).[10] As nucleated cells, nRBC will be automatically included by automated veterinary analyzers in the TNCC and not differentiated as nRBC and thus will increase total WBC counts artifactually. Therefore, nRBC should be enumerated as a percentage during blood film review. Correction of the total WBC count is recommended when nRBC account for more than 5% of the TNCC (see Methods section). Newer technology in automated analyzers shows promise for identifying the presence of nRBC and bands.[118]

Lymphocytes. Lymphocytes are the predominant leukocyte in most strains of healthy wild-type mice, making up 70% to 80% of the WBC differential count.[37,87,119] They are typically 10 to 15 µm in diameter with scant blue cytoplasm, a smooth chromatin pattern, and a round, oval, or slightly indented central nucleus (Figure 2 I).[37,56,87] However, lymphocyte morphology can vary even in health, and variants include larger forms with more dispersed chromatin patterns and increased cytoplasm, which ranges from pale to dark blue and can include azurophilic granules (large granular lymphocytes).[87]

In mice, lymphocyte counts can decrease with handling or other stressors[135] and with age as neutrophil counts increase,[66,119] again demonstrating the need for strain- and age-matched controls in all studies. Vacuolated lymphocytes can be seen in murine lysosomal storage disease models including juvenile neuronal ceroid lipofuscinosis (Figure 2 J, K), sialic acid storage disease, mannosidosis, and Pompe disease[63,95,124,147,178] as well as in chronic active inflammation with lipidosis.[17] The numbers of activated lymphocytes (Figure 2 H) and large granular lymphocytes in circulation can increase due to lymphoma or leukemia, immune

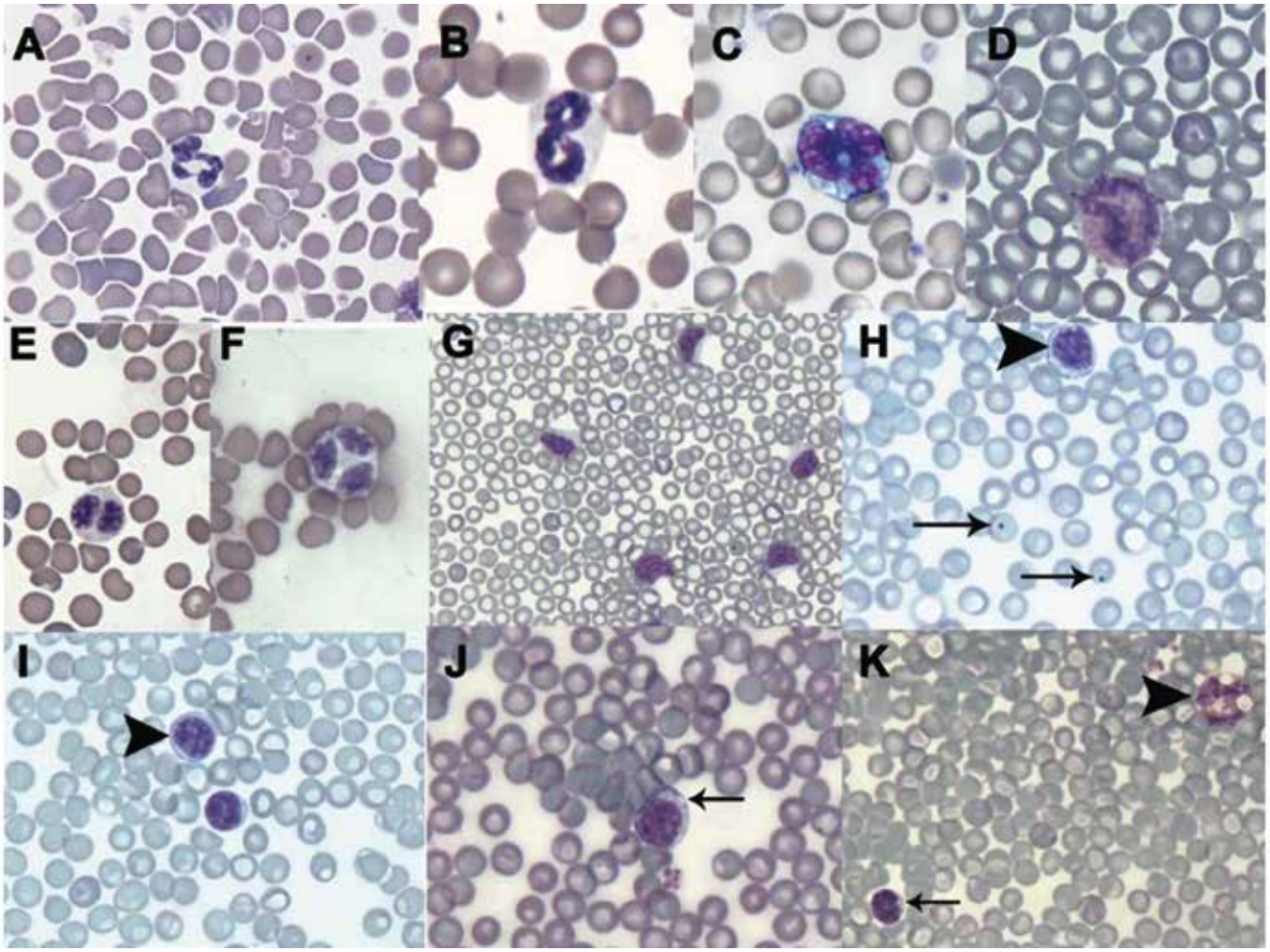

Figure 2. Features of mouse peripheral blood leukocytes: WBC morphologies. (A) Normal mature neutrophil (segmented neutrophil), characterized by faint, finely granular cytoplasm and dense chromatin. (B) 'Figure-8' segmented neutrophil, a common finding in peripheral mouse blood. (C) Ringform monocyte, characterized by abundant pale blue-gray cytoplasm, open chromatin pattern, and cytoplasmic vacuoles. (D) Ringform eosinophil, characterized by multilobed nucleus with typical dense chromatin pattern and abundant eosinophilic cytoplasmic granules. (E) Pseudo-Pelger–Huet-type anomaly in a mouse with myelodysplasia (*Xist*$^{-/-}$), showing hyposegmented nucleus with mature dense chromatin in a neutrophil. (F) Atypical trilobed leukocyte in a mouse with myelodysplasia (*Xist*$^{-/-}$). (G) Circulating lymphoblasts representative of lymphoid leukemia in an aged mouse. (H) Reactive lymphocyte (arrowhead) and Howell–Jolly bodies (arrows) in erythrocytes; the presence of low numbers of Howell–Jolly bodies is considered a normal finding. I. A reactive lymphocyte (arrowhead) in comparison to a normal small lymphocyte. (J) Vacuolated lymphocyte (arrow indicates a vacuole) in a murine model of juvenile neuronal ceroid lipofuscinosis. (K) Vacuolated lymphocyte (arrow) and eosinophil (arrowhead) in a mouse model of juvenile neuronal ceroid lipofuscinosis. Wright–Giemsa staining; original magnification, ×100.

stimulation, and some viral infections,[108,177] and circulating lymphoblasts can be seen with lymphoid leukemia in aged mice (Figure 2 G).

Neutrophils. Neutrophils generally comprise 20% to 30%[119] of the WBC count in mice and are the most common granulocyte. Specific morphologic characteristics include pale, finely granular cytoplasm and a segmented nucleus with areas of both pale and condensed chromatin (Figure 2 A). Unique features of mouse neutrophils include ringform and 'figure 8' nuclei (Figure 2 B)[10,114] and high numbers (5 or 6) of nuclear indentations, which can be interpreted mistakenly as hypersegmentation.[119] Neutrophils have a small storage pool and a 7- to 10-h circulating halflife.[6] Once released from the bone marrow, neutrophils are allocated into the marginal pool and the circulating pool; the circulating pool is included in the leukocyte count. The proportion of neutrophils in the marginal compared with the circulating pool varies by mouse strain.[79,144] The circulating neutrophil count depends on the rate of their release from the bone marrow, the distribution between the marginal and circulating pools, and the rate of migration into tissue.[144]

Increased neutrophil counts (neutrophilia) are associated with responses to stress or excitement[135] and infectious diseases, and typically increase in cases of bacterial infection and acute inflammation[16,17,38,88] given their primary phagocytic and microbiocidal roles. Neutrophil counts can also increase during myeloproliferative disease and myelo- and myelomonocytic leukemia.[174] Due to the small storage pool of neutrophils, both immature and toxic neutrophils may circulate during inflammatory diseases. Immature neutrophils have band or horseshoe-shaped nuclei (that is, nuclei are not yet lobulated); band cells typically are larger than are mature neutrophils. Dysplastic changes include cytoplasmic hypogranulation, bizarre granulation, nuclear hyposegmentation

and bilobation (pseudo-Pelger–Huet anomaly, Figure 2 E), and atypical chromatin condensation.[2,27,125,140,174] In addition, a spontaneous mutant mouse model (mouse ichthyosis) of Pelger–Huet anomaly with a laminin B receptor gene mutation, is similar to that detected in the human disease.[143] The immature neutrophils seen during inflammation can include both bands and young forms such as metamyelocytes and myelocytes, with less mature forms being consecutively less abundant.[144] Bone marrow is the predominant site for increased granulopoiesis during acute inflammation, whereas the spleen is the predominant site for increased erythropoiesis during acute erythropoietic responses.[17,37] The main growth factors for neutrophils include GM-CSF and G-CSF, and their primary chemoattractants include the IL8 homologs MIP2, LIX, and KC.[37,60,81,86,117]

Eosinophils. Eosinophils are granulocytes that are characterized by bright orange to red, round, cytoplasmic granules that are uniformly sized with indistinct borders.[119] These cells generally comprise 0% to 7% of the murine WBC differential count.[119] The nuclei of mature eosinophils typically are multilobulated with condensed chromatin and can be ringform (Figure 2 D). Immature eosinophils are band in form. Eosinophils are involved in parasitic and allergic reactions, and their counts are increased in some GEM models of neoplasia, including chronic eosinophilic leukemia.[173] IL5 is thought to function as their main growth factor and eotaxin as their primary chemoattractant.[37,173] The cytoplasm of eosinophils contains discrete vacuoles in mice with juvenile neuronal ceroid lipofuscinosis (Figure 2 K).

Basophils. Basophils are rare in mice; these cells have few but large, round, deeply basophilic cytoplasmic granules and segmented nuclei. Basophils, like eosinophils, increase in number during parasitic and allergic responses.[44,166] Basophils must be differentiated from mast cells, which occasionally are present in the circulation of mice with inflammatory disease, necrosis, tissue injury, or severe regenerative anemia.[65] Mast cells are larger than are basophils and have round, nonsegmented nuclear morphology and more dense metachromatic cytoplasmic granules (Figure 3 C).[66,166] Basophil counts may be increased when blood is collected from the tail, as the cells are squeezed from the tissue into the blood during collection.[100] IL3 is the primary growth factor[37] for basophils, and they produce IL4.[98,136]

Monocytes. Monocytes are the largest leukocyte and typically make up less than 2% of the total WBC count in mice.[100] However, automated analyzers may undercount this population of cells, and values should be verified by manual review of blood films.[4,6,17,53,,113,145] Monocytes are characterized by their abundant pale gray-blue cytoplasm which often contains vacuoles and occasional faintly eosinophilic granules; nuclei have loose chromatin and are generally bi- or trilobed, reniform, or horseshoe-shaped.[37,87] Monocytes can, also display ringform nuclear morphology (Figure 2C).[10] Mouse monocytes have a 17-h halflife in circulation; 40% of the population of peripheral blood monocytes is circulating, whereas 60% of monocytes are marginated.[37,85,160] The main monocyte growth factors are M-CSF, GM-CSF, and IL3,[37,85] and MCP1 is a primary chemoattractant.[32] Monocytes are a major source of cytokines in the blood, including IL1β, TNFα, and IL6, and monocytosis has been associated with intracellular bacterial infections,[29] chronic inflammation,[16,17,141,166] and neoplasia.[174] Monocytosis also occurs with experimental hemoparasitism, such as trypanosomiasis and malaria,[30,111] and with viral infections, as with mouse cytomegalovirus.[141] Immature forms and promonocytes can be seen during neoplastic conditions.[174] When present on freshly prepared blood films, hemophagocytosis should be noted and may accompany monocytosis, neoplastic disease,[174] or hemolytic anemia. Circulating immature monocytes should be differentiated as part of the phenotypic description of disease models.[174]

Platelets in health and disease. Compared with other mammals, mice have very high platelet counts (900,000 to 1,600,000 per microliter).[37,100,119] Platelet activation in mice can be spontaneous and strain-dependent.[37] Adenosine diphosphate, collagen, arachidonate, and thrombin are potent agonists of platelet clumping in mice.[23] Platelets originate from megakaryocytes in the bone marrow and spleen of mice, and their primary growth factor is thrombopoietin, which is predominantly produced in the liver.[21,103,104,122,149] The lifespan of platelets in mice, approximately 5 d, is shorter than that in other species.[23,37] Automated analyzers often underestimate platelets counts in mice, due to both the small size of platelets and their propensity to clump (Figure 3 D).[37,87] For example, one analyzer (the Advia 120) may falsely report platelet clumps as eosinophils, because the highly variable size and granularity of these clumps cause them to appear as a heterogenous population in the area of the dot plot where eosinophils normally appear. As for other veterinary species, the feathered edge of a blood film (Figure 1 A) should be scanned for platelet clumps to aid in judging the accuracy of automated platelet counts in mice.

On blood films, mouse platelets are 1 to 4 µm in diameter, anucleate, with discoid, spheroid, or elongated or spindloid morphology, and central basophilic, eosinophilic, or metachromatic granules scattered throughout faintly pink to gray cytoplasm.[37,87,119] Cell membranes may have a few fine threadlike surface projections. Both mature and reticulated (young) platelets can be counted by flow cytometry.[119,130] In addition, mice may have circulating giant or megaplatelets, described as such when they are equal in size to or larger than an RBC, respectively (Figure 1 F, G). Giant platelets increase in number in response to accelerated hematopoiesis; this morphology can be correlated with an increased MPV.[66]

The main function of platelets is primary hemostasis, and platelet production can increase due to inflammatory disease, myeloproliferative disease and neoplasia, and iron deficiency.[57,119,138] Conversely, platelet production can decrease due to myeloproliferative disease, neoplasia, and erythropoietin administration and in various GEM models.[58,97,125] Dysplastic changes, including retained nuclei, circulating micromegakaryocytes,[76] and atypical cytoplasmic granulation,[174] are associated with myeloproliferative disorders, for example. Giant and megaplatelets can occur with leukemias, myelofibrosis, thrombocythemia, and polycythemia vera[83,139,174] and are released from the bone marrow in response to thrombocytopenia and when the peripheral blood halflife of normal circulating platelets is decreased (Figure 1 F, G).[37] Populations of giant and megaplatelets as well as microcytic and fragmented erythrocytes can overlap in automated analyzers that sort cells according to size, thus skewing both cell counts (Figure 4 E).[75,152] The MPV is a sensitive indicator of increased platelet production and increases in response to hypoxia-induced thrombocytopenia[70,97] and various genetically or physiologically induced causes of thrombocytopenia.[23]

Other cells. Circulating mast cells (Figure 3 C) occur occasionally, depending on the blood collection site, and must be differentiated from basophils (described earlier). In addition, epithelial

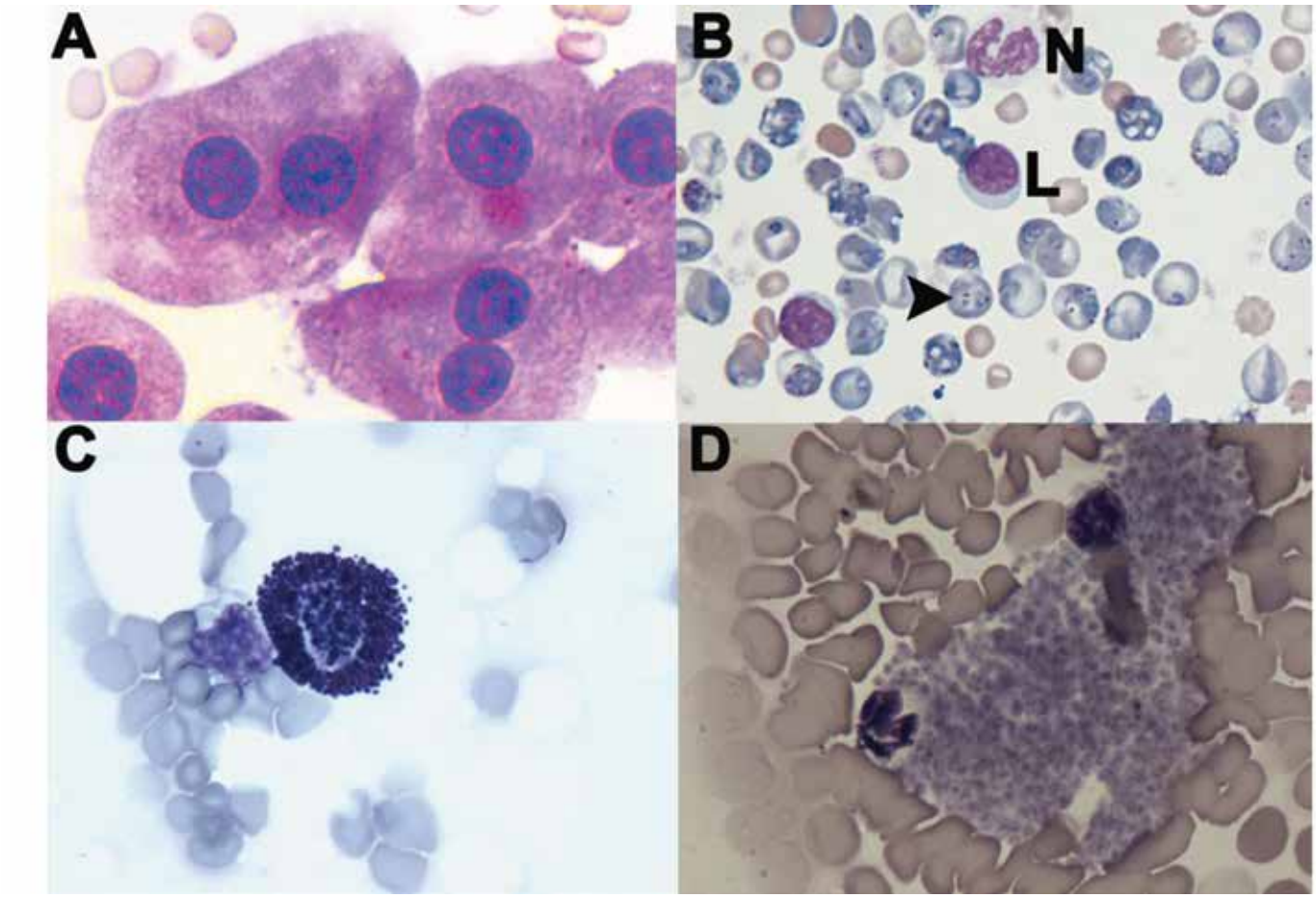

Figure 3. Other cells that can be seen in mouse blood films. (A) Hepatocytes on feathered edge after aspiration of liver during cardiocentesis. (B) *Plasmodium* sp (arrowhead) infecting approximately 50% of erythrocytes and markedly increased polychromasia in an anemic mouse; mouse model of malaria. There are also lymphocytes (L) and a neutrophil (N) in this field. (C) Mast cell (atypical finding in mouse peripheral blood) at feathered edge. (D) Large platelet clump at the feathered edge; automated platelet counts will be artifactually low due to clumping. Wright–Giemsa staining; original magnification, ×100.

cells can be seen secondary to a poorly performed cardiac puncture when other internal organs are aspirated inadvertently. For example, when the liver is aspirated during cardiocentesis, hepatocytes might collect along the feathered edge of the blood film (Figure 3 A). Furthermore, blood parasites sometimes are present in blood films from various mouse models with infections such as malaria (Figure 3 B), babesiosis, and trypanosomiasis.[12,52,92]

Automated Methods in Mouse Hematology

Several options are available for automated veterinary analyzers, including impedance, laser, and combination instruments. Given the cellular differences we already have described, human automated analyzers will not provide accurate results for mice. Although veterinary analyzers are more often evaluated and reviewed for companion animal medicine,[7,74,113] both Bayer (Tarrytown, New York) and Abbott (Abbott Park, Illinois) have software for WBC differentiation for mice,[37] and Heska (Loveland, Colorado) and Idexx (Westbrook, Maine) have recently added mouse-specific software and microvolume sample options (Figure 4 A–C). Instrument operators must be trained in maintenance procedures, error flags, troubleshooting, and appropriate quality control,[168] and instruments should go through a standardized validation procedure and be compared with a 'gold-standard' method, such as a manual method or a previously validated instrument.[50,91,161] The leukocyte differential is one component of the automated CBC analysis that has still not replaced manual methods as the gold standard in veterinary medicine.[161] Mice have several physiologic variables that may decrease the efficacy of automated analyses including small RBC, relatively high numbers of circulating immature and nucleated RBC, variable leukocyte morphology, and platelet clumping. Therefore, manual leukocyte differential and blood-film review are still warranted. In addition to these physiologic factors, the mouse's utility for biomedical research includes the ease with which its physiology and genetics can be manipulated. These manipulations can lead to unpredictable changes in hematologic variables; therefore it is important to consult a blinded, well-trained observer familiar with veterinary, and particularly murine, clinical pathology to detect and appropriately interpret changes in blood cell counts and indices, distribution, and morphology by using appropriately matched controls.

Genetic mutations, iron deficiency, and inflammatory disease are examples of disorders that can cause changes in cell morphology or size, thus resulting in overlap of various cell populations by automated analyzers. Therefore, evaluating not only a blood

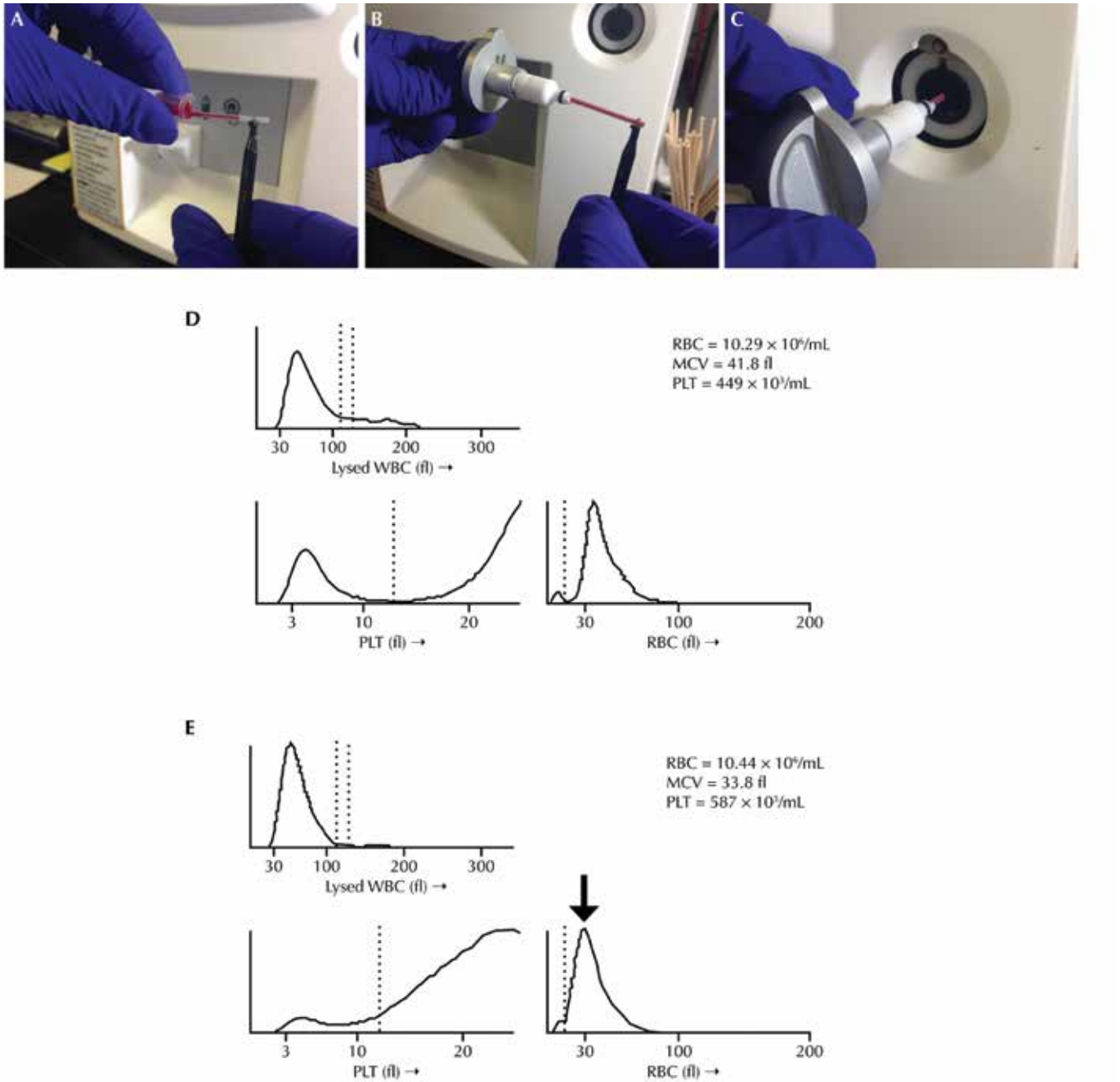

Figure 4. Features of an automated analyzer, the Heska Hematrue. The manual micropipette adapter (MPA, 20 µL) enables analysis of small volume blood samples. Using the MPA, blood is withdrawn by capillary action into (A) a specialized microhematocrit tube held by provided forceps. The microhematocrit tube then is placed into the (B) MPA device and inserted into (C) the MPA holder. The analyzer prints cellular histograms showing 3 populations (WBC, RBC, and platelets) for evaluation and comparison with results from review of blood films. (D) Histograms from a naïve C57Bl/6 mouse sample showing normocytic RBC with an MCV of 41.8 fl. (E) Histograms from an anemic transgenic iron-deficient mouse (*tmprss6* $^{-/-}$), showing a microcytic RBC population (shifted left on the *x* axis) with an MCV of 33.8 fl.

film but also instrument-generated cell-population histograms (Figure 4 D, E) becomes necessary.[23,168] Previous studies show that markedly microcytic or fragmented erythrocytes (as well as other cell debris) can overlap with the size-based platelet population,[17,43,152,168] thus skewing both RBC and platelet counts (Figure 4 E). Results from automated analyzers should always be verified by manual blood film review, especially when the automated analyzer reports atypically high or low values.

Methods for Collecting Quality Samples and Analysis of Bone Marrow

Collection for cytology. The optimal method for generating samples for mouse bone-marrow cytology is the brush preparation. When properly performed, this method preserves cellular morphology without dilutional or mechanically induced cellular damage. Samples should be collected immediately postmortem

from the sternum or femur.[127] Briefly, to allow maximal exposure of the marrow, the bone (usually the femur, for the most sample) is bisected lengthwise by using a clean razor or surgical blade. A small paintbrush dampened with PBS is gently brushed along the marrow surface to collect the cells. Then the collected cells are brushed gently lengthwise along a slide in long rows, as the brush is rotated for each row to deposit the cells in a monolayer[37,156](Figure 5 A). Other methods of slide preparation include push slides, squash preps, and cytocentrifugation, in which the marrow is flushed similar to preparation for flow cytometric evaluation,[127] however, these methods often result in increased numbers of broken and smeared cells, which cannot be evaluated. Bone marrow slides can be stained routinely with Wright–Giemsa, Giemsa, or Prussian blue for evaluation by light microscopy and are generally stained twice as long as peripheral blood films.[156,168] Cellularity and morphology will be excellent when gentle handling is used.

Collection for histology. Bone marrow from the sternum, vertebrae, humerus, or femur can be collected for histology,[36,127] and consistency of site collection is recommended for best comparison within or between studies. Samples collected at necropsy should be fixed as soon as possible (within 20 min) in 10% neutral buffered formalin or Bouin solution and decalcified in a chelating agent (for example, EDTA) or a weak organic acid.[127,156] Excess decalcification should be avoided to preserve cellular morphology and when sections are to be used for special staining. Alternatively decalcification may be unnecessary before sectioning very small bones. Sections are processed routinely through graded alcohols and embedded in paraffin; 3- to 4-µm tissue sections are recommended for the best cellular detail. Slides then can be stained with hematoxylin and eosin and special stains (discussed later). Bone marrow histology is most useful for assessing architecture, overall cellularity, neoplastic infiltrates, and myelofibrosis.

Collection for flow cytometry. Flow cytometric analysis can be a useful adjunct to morphologic assessments. The femur is the typical collection site for flow cytometry, allowing for 10 to 30 million cells from a single bone.[23,130] Once the femur is dissected, both ends can be removed by using a razor. A 12-mL syringe is filled with buffer and, with a 21- to 23-gauge needle attached, is inserted into one end of the femur and flushed by using alternating fast and slow pulses to maximize cell yield. Flow cytometric analyses must be performed immediately after cell collection.[127] These analyses are beyond the scope of this paper but have been reviewed recently.[31,90,127,170] As with most aspects of phenotypic characterization, flow cytometric parameters can vary with mouse strain and other preanalytic factors.[112]

Cytochemical Staining of Blood and Bone Marrow

Routine staining for bone marrow and blood includes use of a Romanowsky-type stain (Figures 1 C, 5 B). Reticulocytes are best visualized and enumerated by NMB staining (Figure 1 D). Polychromasia can be estimated from Wright–Giemsa-stained preparations (Figure 1 C).[28] In mouse bone marrow (and peripheral blood with certain manipulations) it can be very challenging to differentiate immature cell types by morphology alone. For example, lymphoblasts, monoblasts, and myeloblasts can overlap in morphologic features, as can atypical or immature cells in cases of myelodysplasia or neoplasia. In some cases, cellular origin cannot be differentiated by routine microscopy, but some cells contain inclusions or storage material that can be used to confirm identification. In such cases, special stains such as periodic acid–Schiff for glycogen inclusions, Masson trichrome for stroma, Prussian blue for iron-positive inclusions (Figure 5 F, G), and reticulin for bone marrow myelofibrosis (Figure 5 H) may be necessary. In addition, unstained slides can be used for other special stains and cytochemical analyses (Figure 6).

Immunocytochemistry and Immunohistochemistry

Immunocytochemistry and immunohistochemistry can be performed on fresh unstained blood or bone marrow slides, destained slides,[93] or histology sections of bone marrow and other tissue. Briefly, slides are fixed with methanol, washed with buffer, and incubated with a protein blocker, then a primary antibody, followed by a secondary antibody, and finally a color-development enzyme solution.[19] Specific antibodies useful in blood and bone marrow samples include those to CD71, Ter119, B220, CD3, CD1b, Gr1, F4/80, Mac2, and CD41.[17,22,80,165,174] Immature forms can be identified by using various combinations of stem cell markers.[25] Additional antibodies useful in the hematopathology of mice using formalin-fixed, paraffin-embedded material are reviewed elsewhere.[77,128] Most antibodies tend to yield higher signals on frozen tissue (avoids the extra steps required for fixed tissues), but frozen samples are suboptimal for assessing tissue and cellular morphology. Although immunocytochemistry and immunohistochemistry provide important diagnostic information, most markers are associated with but are not specific for various cell lineages, so panels are often required for cell identification, and concurrent control samples from age-, sex-, strain-, and disease-matched mice are needed.

Bone Marrow: General Considerations and Responses to Disease

Bone marrow cytologic evaluation is needed to determine the myeloid:erythroid ratio, to differentiate hematopoietic precursors, characterize changes in bone marrow hematopoiesis relative to peripheral blood cell counts, assess individual cell morphology, differentiate lymphoid and erythroid cells, and assess features of myelodysplasia or neoplasia.[127] In addition, bone marrow is evaluated by histopathology to assess overall cellularity and architecture and to identify necrosis, inflammation, or infiltrative disease.[127,156] Collection sites should remain consistent within and between experiments (see Methods), and concurrent controls are needed. Bone marrow cytology is especially useful when circulating atypical cells have been detected and when erythrocyte indices suggest abnormal hematopoiesis.[127] Wright–Giemsa-stained preparations are best evaluated by using the 100× objective to assess cellular morphologic detail including megakaryocytes (Figure 5 C, D) and to determine the myeloid:erythroid ratio and cellular percentages (Figure 5 B, I).[87] At least 500 cells should be counted and classified by type—including myeloid (granulocytic and monocytic), erythroid, and megakaryocytic lineages as well as lymphocytes, macrophages, plasma cells, mast cells—and cellular stage of maturation.[156] Slides should be prepared concurrently from appropriate controls to evaluate for hematopathology. For complete hematologic evaluation in in mice, bone marrow cytologic evaluation is performed as an adjunct to peripheral

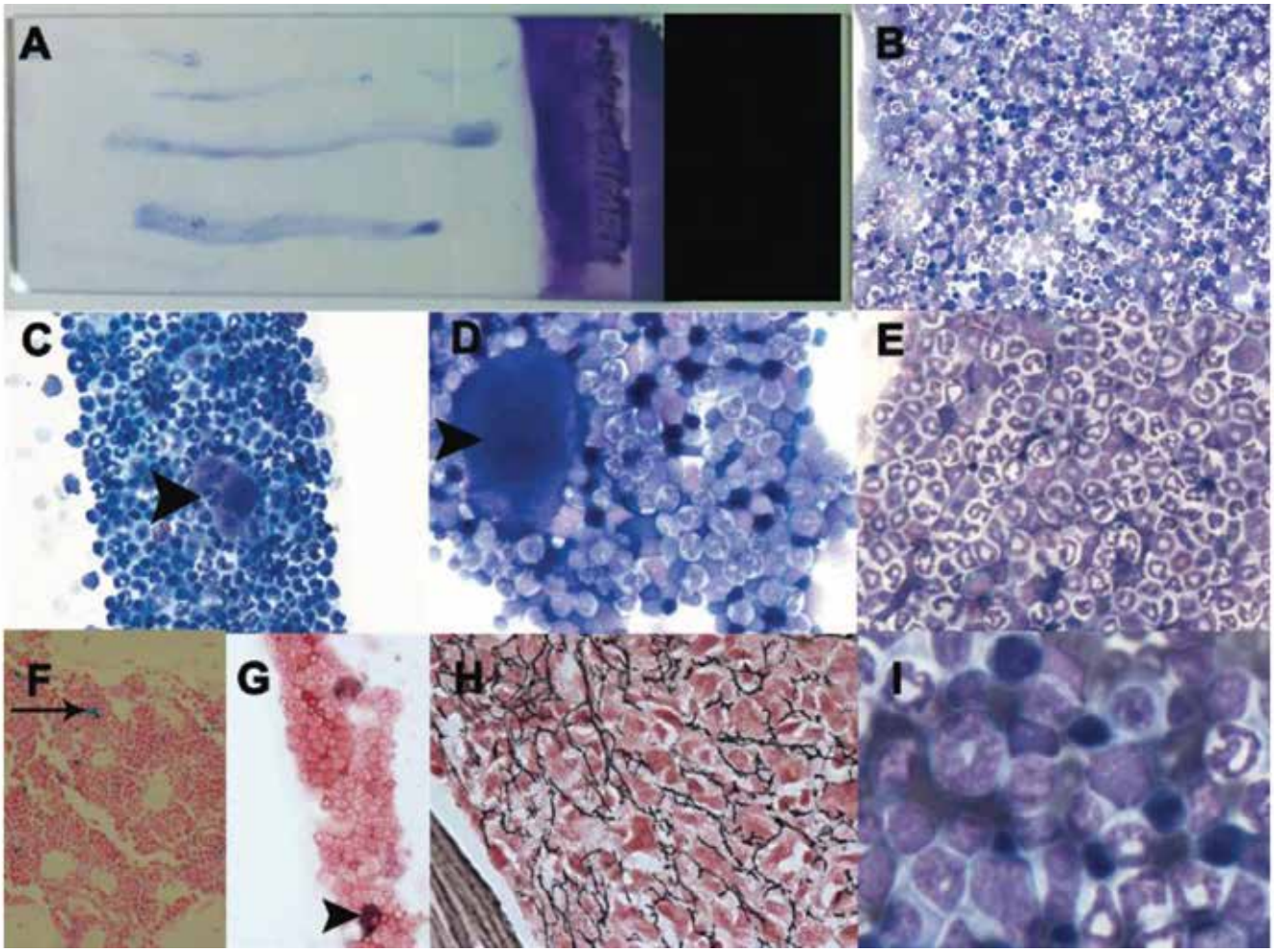

Figure 5. Features of mouse bone marrow. (A) Representative slide resulting from the 'brush preparation' method for bone marrow cytology. (B) Mouse bone marrow sample with normal cellularity and myeloid:erythroid ratio (approximately 1:1 in this case). Wright–Giemsa staining; original magnification, ×50. (C) Empiropolesis of a neutrophil (arrow) through a megakaryocyte, a common finding in mouse bone marrow. Wright–Giemsa staining; original magnification, ×50. (D) Typical megakaryocyte (arrowhead), characterized by multilobulated nucleus with dense chromatin pattern and abundant medium-blue cytoplasm. Wright–Giemsa staining; original magnification, 100×. (E) Myeloid hyperplasia (increased myeloid:erythroid ratio, approximately 7:1 in this case), characterized by increased numbers of mature neutrophils; bone marrow cytology from a colony mouse with cervical lymphadenitis. Wright–Giemsa staining; original magnification, ×100. (F) Formalin-fixed, paraffin-embedded bone marrow from control mouse showing iron-containing macrophages (arrow). Prussian blue staining; original magnification, ×20. (G) Bone marrow from control mouse showing macrophages (arrowhead) containing iron as hemosiderin. Prussian blue staining; original magnification, ×50. (H) Markedly increased reticulin staining (myelofibrosis, black fibers) in formalin-fixed, paraffin-embedded bone marrow from a 9-mo-old mouse with myeloproliferative disease (*Xist*–/–). Original magnification, ×60. (I) Close-up of normal mouse bone marrow, showing typical ringform neutrophils and their precursors and erythroid precursors (darker cells). Wright–Giemsa staining; original magnification, ×100.

blood assessment (CBC and blood film review), bone marrow histology, and histopathology of the spleen.[17,127,153] Special stains used for mouse blood and bone marrow are outlined in Figure 6. In general, bone marrow cellularity is higher for mice than for other species, with as much as 90% to 95% of medullary space in the femur and vertebral column occupied by marrow;[100,130] strain- and age-associated variability is best identified by the evaluation of concurrent controls and by using consistent collection sites. The detailed architecture of murine bone marrow has been reviewed.[154] Flow cytometry is a useful adjunct to detailed morphologic assessment of the bone marrow, especially when multiple cell-surface markers are used.[31,90,127,170]

The normal myeloid:erythroid ratio in mice ranges from 0.8 to 2.8:1 (average, 1.5:1),[37] and age and strain must be considered during comparative analyses. The nuclei and cytoplasm should mature together, asynchronous maturation is abnormal, and cellular maturation should be complete and orderly for all lineages. Megakaryocyte emperipolesis (the passage of an intact leukocyte through another cell) is considered a normal finding and is common in bone marrow from mice (Figure 5 C).[119] Bone marrow cellularity tends to increase with inflammatory disease (Figure 5 E) and age. However, functional capacity declines with age, and myelofibrosis (fibro-osseous lesions) can occur in mice before they are 2 y of age.[129,151] This abnormality is more common in female than male mice and may represent an estrogenic effect.[46,132,163] In addition, myelofibrosis can be an important feature of bone marrow disease in younger, especially genetically manipulated, mice.[73,83,174] As in human hematopathology practice, identification

Stain	Use	References	
		Cytology	Histology
Wright–Giemsa	Best for morphologic evaluation of blood and bone marrow. Immature RBC appear light blue (polychromatophilic) due to dispersed RNA still present in the cytoplasm; bacteria are dark blue.		
Giemsa	Bacterial organisms on histology; adjunct to seeing erythroid cells in cytology or histology.		
Diff-Quick	Hematology; variable staining of mast cell granules if dysplastic or neoplastic.		
New methylene blue (NMB)	Supravital stain that is best for reticulocytes and Heinz bodies. Dye causes precipitation of rRNA and organelles into a reticulum seen as clumped aggregates of dark-blue material.	62	
Toluidine blue	Basic dye that reacts with acid mucopolysaccharides in mast cell granules to form metachromatic complexes that appear red-purple. Helpful for evaluation of basophil and mast cell populations.	126	34
Periodic acid–Schiff (PAS)	Differentiates granulocytic and megakaryocytic precursors (which stain more intensely) from lymphoid precursors; also used to detect erythroid precursors.	173	69
Masson trichrome	Sequential staining method involving iron hematoxylin (stains nuclei black), Biebrich scarlet (stains cytoplasm red), and aniline blue or aniline light green (stains collagen in tissues blue or green, respectively).		5
Prussian blue	Useful in bone marrow and blood to detect siderocytes and ring sideroblasts containing iron as hemosiderin. Staining intensity can be scored subjectively on a scale of 0 to 4 under light microscopy. Useful to assess splenic iron stores, especially during states of anemia and inflammatory disease. Iron is primarily stored in mouse splenic red pulp, and interstrain differences in iron trafficking are reported.	16, 173	16, 47
Reticulin	Stains reticulin fibers made of collagen III; particularly useful in bone marrow sections to detect myelofibrosis.	173	102

Figure 6. Examples of common cytochemical stains and their uses for mouse bone marrow.

and grading of myelofibrosis in murine bone marrow by using slides stained with reticulin (Figure 5 H) or trichrome (for type I collagen) can be helpful in the assessment of disease.[78,174] Adipose tissue often increases concurrently with decreasing marrow cellularity, and indeed, adipocytes have been shown to suppress hematopoiesis in mice.[107,154] Importantly, hematopoietic neoplasia occurs with relatively high frequency in different strains of aging mice (Figure 2 G), and this fact must be considered carefully when attempting to differentiate a neoplastic phenotype from a strain-related background lesion and to characterize such neoplasms correctly.[14,77] New genetic mutations are being discovered or induced in mice at an ever-increasing rate, and many of these have important direct or indirect effects on hematopoietic development, can cause immunosuppression, and that must be considered in the context of the background strain when interpreting bone marrow findings.[1,137,171]

Erythroid lineage. Erythropoiesis begins in erythroblastic islands, which consist of a central 'nurse' macrophage surrounded by RBC at various stages of differentiation. Rubriblasts are large cells with large round nuclei, finely stippled and reddish chromatin, nucleoli, and a narrow rim of deeply basophilic cytoplasm. The next stage of maturation is the prorubricyte, with more coarse chromatin, and loss of nucleoli. Rubricytes are the most mature stage capable of mitosis. These cells are smaller than the earlier forms, with very coarse chromatin and light blue to gray cytoplasm (Figure 5 I). Metarubricytes are smaller than rubricytes, with a pyknotic nucleus and polychromatic cytoplasm. Removal of the nucleus from metarubricytes leads to the formation of polychromatophilic erythrocytes, which are reticulocytes that contain aggregates of RNA which stain with NMB. The final stage of erythroid maturation is the mature erythrocyte, which is anucleate and has pink to red hemoglobinized cytoplasm.[156] In human medicine, the term 'normoblast' is used for RBC precursors, with pronormoblasts roughly equivalent to rubriblasts, basophilic normoblasts to prorubricytes, polychromatophilic normoblasts to rubricytes, and orthochromatic normoblasts to metarubricytes.[49] Erythroid precursors can comprise 20% to 50% of the TNCC in bone marrow, and with normal maturation, the more mature forms are present in greater numbers than are immature forms. The primary erythroid growth factor is erythropoietin, a protein secreted by the kidneys.[37,156] Dysplastic changes of erythroid cells include binucleate precursors, siderocytes and ring sideroblasts, nuclear cytoplasmic asynchrony, and atypical mitoses.[125,159,174] Orderly, progressive maturation or maturation arrest should be assessed and blast percentages enumerated as part of an evaluation for myeloproliferative neoplasia.

Myeloid lineage. The granulocytic myeloid lineage normally progresses from myeloblast (early stage) to promyelocyte, myelocyte, and then metamyelocyte.[169] Band neutrophils and segmented neutrophils (most mature stage) predominate in normal maturation (Figure 5 I). The monocytic myeloid lineage starts with the same bipotential granulocyte–macrophage colony-forming unit (CFU-GM) as for the granulocytic lineage but then is influenced by IL3, GM-CSF, and M-CSF to accomplish monoblastic differentiation.[9,85] Promonocytes develop with cytoplasmic vacuolation and irregular cell membranes. Myeloid precursors account for 30% to 50% of the TNCC in bone marrow. Mature forms should outnumber immature forms, with blasts

comprising 2% of the total myeloid component.[87] Increased blasts may indicate neoplasia of either the myeloid or lymphoid lineage.[128] Ring forms can be present starting at the promyelocyte stage in neutrophils and eosinophils and in the monocyte lineage. Myeloid hyperplasia can occur during infectious disease and myeloproliferative disease.[16,174] Histiocytic sarcoma is a common tumor of aging mice and is characterized by sheets of round to elongate cells with abundant variably foamy eosinophilic cytoplasm, vesiculate nuclei, and prominent nucleoli.[55] Erythrophagocytosis and multinucleated giant cells can occur with infiltrative histiocytic sarcoma of the bone marrow and spleen[164,174] and with other lympho- or myeloproliferative neoplastic and inflammatory diseases including granulomatous diseases[67] and intracellular bacterial infections such as salmonellosis.[16,17,96]

Megakaryocytes. Megakaryopoiesis occurs adjacent to the sinus endothelium.[156] Megakaryocytes are platelet precursors and form in the bone marrow first as megakaryoblasts, which are large with 1 to 4 reddish nuclei and a small amount of deeply basophilic cytoplasm. These then progress to promegakaryocytes, in which nuclei multiply and may fuse into a common mass with a narrow rim of cytoplasm; finally, megakaryocytes are formed (Figure 5 D). Megakaryocytes are the largest (20 to 160 µm diameter) hematopoietic precursors in the bone marrow. They are usually round, with a single, multilobed nuclear mass, abundant pale cytoplasm, and numerous small azurophilic granules. There are about twice as many megakaryocytes in adult mouse bone marrow as compared with human.[134] Dysplastic changes include hypolobation, atypical mitoses, small forms, and clustering.[35,150,174] Mouse megakaryocytes typically have 16 nuclei, but this count varies by strain.[65,134]

Other cells. Lymphocytes are more abundant (7% to 21% of nucleated cells) in the bone marrow of mice than other species,[119] and small lymphocytes predominate. Young mice may have increased numbers of lymphocytes; bone marrow lymphocyte density does not correlate well with peripheral blood lymphocyte counts[127] and may vary by age, sex, strain, and GEM. Although distinguishing lymphoid from erythroid cells in histologic sections can be difficult, mouse-specific lymphoid and erythroid markers are available for immunohistochemistry.[128] Erythroid cells can be identified in mice by using the Ter119 antibody.[146,174] Lymphoblasts are present in low numbers (less than 2%) in normal mice, and immunohistochemistry or flow cytometry can be helpful in differentiating cell lineages.[31,172] Other cells normally present in low numbers in the bone marrow of mice include macrophages, plasma cells, osteoclasts, mast cells, and endothelial cells. Bone marrow macrophages are often phagocytic and notably increase in various infectious diseases[16,17] and neoplastic conditions.[77,174] Plasma cells, which should account for less than 3% of the TNCC, are round to oval, with abundant deeply basophilic cytoplasm and round eccentric nuclei with a perinuclear clear zone, and the cytoplasm may be filled with Russell bodies (immunoglobulins).[87,172] Osteoclasts are large irregular cells with multiple oval nuclei and pink granular cytoplasm, which may increase with bone remodeling, changes in hormone and vitamin D levels, and sarcomas.[18,44,54] Osteoclasts can be differentiated from megakaryocytes by the separated nuclei (as compared with as a single mass) and more open chromatin pattern of osteoclasts. Mast cell percentages can increase during innate immune responses and neutrophil recruitment.[45] Both osteoclast and mast cell numbers in the bone marrow vary with mouse strain.[45,106]

Splenic Extramedullary Hematopoiesis

Because the major hematopoietic tissues of mice include bone marrow, spleen, and, to a lesser extent, liver,[37,114,153] analysis of these tissues should be included with CBC and blood film review for complete hematologic evaluation in this species. The spleen is the primary site for iron storage in mice,[114,153] but the iron storage amounts vary by strain.[47] Splenic extramedullary hematopoiesis persists throughout life in normal mice and comprises about 30% of hematopoiesis[114,130]. Splenic extramedullary hematopoiesis produces all 3 hematopoietic lineages: myeloid precursors, erythroid precursors, and megakaryocytes.[153] This degree of splenic extramedullary hematopoiesis is unique to rodents and is an important consideration in regard to comparative pathology when developing or assessing mouse models of human disease.[175] Under normal conditions, low levels of extramedullary hematopoiesis may occur in the liver as well as other sites, including lymph nodes.[68,73,167] Lymphoma, histiocytic sarcoma, mast cell tumor, hemangioma and hemangiosarcoma, and leukemia can occur in the spleens of rodents.[153] Whether from anemia, inflammatory disease, altered iron trafficking, storage disease, or other pathologies, marked splenomegaly is a unique and common response to increased hematopoiesis in mice and should not be misconstrued as a neoplastic phenomenon only.[16,17,24,47,99,147,153,174] In general, the spleen is the primary responding tissue for increased erythropoiesis, whereas the bone marrow is the main responder for myelopoiesis.[17,37,167]

Conclusions

Herein we have reviewed murine hematology and provided examples of important hematopathologic responses in mice, thus demonstrating the value of complete murine hematologic analyses during biomedical research. An important component of biomedical research is the potential translation of findings to human and veterinary medicine. Appropriately designed studies with correct and consistent sample collection and evaluation and relevant controls support the elucidation of important phenotypes, hematopathologies, and responsiveness to investigational therapeutics. Blinded observations, randomization,[115] and studies designed with appropriate statistical power[42] enhance the quality of research and allow for repeatability and subsequent translation of important findings. A strategic plan for hematologic analyses in mouse models should include the evaluation of GEM and other disease models for both expected and unexpected hematologic phenotypes.

High-quality hematologic analyses for laboratory mice are possible and practical and can provide insight into the phenotypes and pathogenesis of mouse models of human and veterinary diseases and the evaluation of responsiveness to novel therapeutic investigations. In this manuscript, we describe various practical methods for the collection and processing of samples for automated and manual analyses and provide examples of the utility of these laboratory tests for modern biomedical research. We hope this article provides a reference framework for improved experimental design, understanding of hematophysiology, interpretation of results and important findings for murine hematologic

studies, and description of important hematopathologic responses and cellular morphologies clearly demonstrable in mouse blood and bone marrow.

Acknowledgments

We thank Carlos Lopez-Otin and Herbert Y Lin for kindly providing the *tmprss6*$^{-/-}$ mice and Susan L Cotman for sharing samples from the juvenile neuronal ceroid lipofuscinosis mice.

References

1. **Aicher A, Heeschen C, Mildner-Rihm C, Urbich C, Ihling C, Technau-Ihling K, Zeiher AM, Dimmeler S.** 2003. Essential role of endothelial nitric oxide synthase for mobilization of stem and progenitor cells. Nat Med **9:**1370–1376.
2. **Alemdehy MF, van Boxtel NGJA, de Looper HWJ, van den Berge IJ, Sanders MA, Cupedo T, Touw IP, Erkeland SJ.** 2012. Dicer 1 depletion in myeloid-committed progenitors causes neutrophil dysplasia and blocks macrophages dendritic cell development in mice. Blood **119:**4723–4730.
3. **Ameri M, Schnaars HA, Sibley JR, Honor DJ**. 2011. Stability of hematologic analytes in monkey, rabbit, rat, and mouse blood stored at 4 °C in EDTA using the ADVIA 120 hematology analyzer. Vet Clin Pathol **40:**188–193.
4. **Arroyo AE, Tabernero MD, García-Marcos MA, Orfeo A.** 2005. Analytic performance of the Pentra 80 automated blood cell analyzer for the evaluation of normal and pathologic WBCs. Am J Clin Pathol **123:**206–214.
5. **Avasarala S, Zhang F, Liu G, Wang R, London SD, London L.** 2013. Curcumin modulates the inflammatory response and inhibits subsequent fibrosis in a mouse model of viral-induced acute respiratory distress syndrome. PLoS ONE **8:**e57285.
6. **Basu S.** 2002. Evaluation of role of G-CSF in the production, survival, and release of neutrophils from bone marrow into circulation. Blood **100:**854–861.
7. **Becker M, Moritz A, Giger U**. 2008. Comparative clinical study of canine and feline total blood cell count results with 7 in-clinic and 2 commercial laboratory hematology analyzers. Vet Clin Pathol **37:**373–384.
8. **Begley DA, Krupke DM, Neuhauser SB, Richardson JE, Bult CJ, Eppig JT, Sundberg JP.** 2012. The Mouse Tumor Biology Database (MTB): a central electronic resource for locating and integrating mouse tumor pathology data. Vet Pathol **49:**218–223.
9. **Bienzle D.** 2000. Monocytes and macrophages, p 318–325. In: Feldman BF, Zinkl JG, Jain NC, editors. Schalm's veterinary hematology. Hoboken (NJ): Wiley–Blackwell.
10. **Biermann H, Pietz B, Dreier R, Schmid K, Sorg C, Sunderkötter C.** 1999. Murine leukocytes with ring-shaped nuclei include granulocytes, monocytes, and their precursors. J Leukoc Biol **65:**217–231.
11. **Blue JT.** 2000. Myelodysplastic syndromes and myelofibrosis, p 682–688. In: Feldman BF, Zinkl JG, Jain NC, editors. Schalm's veterinary hematology. Hoboken (NJ): Wiley–Blackwell.
12. **Borggraefe I, Yuan J, Telford SR 3rd, Menon S, Hunter R, Shah S, Spielman A, Gelfand JA, Wortis HH, Vannier E.** 2006. *Babesia microti* primarily invades mature erythrocytes in mice. Infect Immun **74:**3204–3212.
13. **Brayton C, Treuting PM.** 2011. Phenotyping, p 7–14. In: Treuting PM, Dintzis SM, editors. Comparative anatomy and histology. Amsterdam (The Netherlands): Elsevier.
14. **Brayton CF, Treuting PM, Ward JM.** 2012. Pathobiology of aging mice and GEM: background strains and experimental design. Vet Pathol **49:**85–105.
15. **Brockus CW.** 2011. Erythrocytes, p. 3–44. In: Latimer KS, editor. Veterinary laboratory medicine: clinical pathology. Hoboken (NJ): Wiley–Blackwell.
16. **Brown DE, Libby SJ, Moreland SM, McCoy MW, Brabb T, Stepanek A, Fang FC, Detweiler CS.** 2013. *Salmonella enterica* causes more severe inflammatory disease in C57/BL6 *Nramp1*^{G169} mice than Sv129S6 mice. Vet Pathol **50:**867–876.
17. **Brown DE, McCoy M, Pilonieta M, Nix R, Detweiler C.** 2010. Chronic murine typhoid fever is a natural model of secondary hemophagocytic lymphohistiocytosis. PLoS ONE **5:**e9441.
18. **Buchwald ZS, Kiesel JR, Yang C, Dipaolo R, Novack DV, Aurora R.** 2013. Osteoclast-induced Foxp3 CD8 T cells limit bone loss in mice. Bone **56:**163–173.
19. **Buchwalow IB, Bèocker W.** 2010. Immunohistochemistry: basics and methods. New York (NY): Springer.
20. **Burkhard MJ, Brown DE, McGrath JP, Meador VP, Mayle DA, Keaton MJ, Hoffman WP, Zimmermann JL, Abbott DL, Sun SC.** 2001. Evaluation of the erythroid regenerative response in 2 different models of experimental iron deficiency anemia. Vet Clin Pathol **30:**76–85.
21. **Burmester H, Wolber E-M, Freitag P, Fandrey J, Jelkmann W.** 2005. Thrombopoietin production in wild-type and interleukin 6 knockout mice with acute inflammation. J Interferon Cytokine Res **25:**407–413.
22. **Burry RW**. 2010. Immunocytochemistry: a practical guide for biomedical research. New York (NY): Springer.
23. **Car BD, Eng VM.** 2001. Special considerations in the evaluation of the hematology and hemostasis of mutant mice. Vet Pathol **38:**20–30.
24. **Carter PR, Watts MN, Kosloski-Davidson M, Prasai K, Grisham MB, Harris NR.** 2013. Iron status, anemia, and plasma erythropoietin levels in acute and chronic mouse models of colitis. Inflamm Bowel Dis **19:**1260–1265.
25. **Challen GA, Boles N, Lin KK, Goodell MA**. 2009. Mouse hematopoietic stem cell identification and analysis. Cytometry Part A **75:**14–24. doi: 10.1002/cyto.a.20674.
26. **Chen W, Sun CC, Chen S, Meynard D, Babitt JL, Lin HY.** 2013. A novel validated enzyme-linked immunosorbent assay to quantify soluble hemojuvelin in mouse serum. Haematologica **98:**296–304.
27. **Colella R, Hollensead SC.** 2012. Understanding and recognizing the Pelger–Huet anomaly. Am J Clin Pathol **137:**358–366.
28. **Collicutt NB, Grindem CB, Neel JA**. 2012. Comparison of manual polychromatophilic cell and automated reticulocyte quantification in evaluating regenerative response in anemic dogs. Vet Clin Pathol **41:**256–260. doi: 10.1111/j.1939-165X.2012.00432.x.
29. **Cooper AM, Flynn JL.** 1995. The protective immune response to *Mycobacterium tuberculosis*. Curr Opin Immunol **7:**512–516.
30. **Cordeiro RS, Cunha FQ, Filho JA, Flores CA, Vasconcelos HN, Martins MA.** 1983. *Plasmodium berghei*: physiopathological changes during infections in mice. Ann Trop Med Parasitol **77:**455–465.
31. **Criswell KA, Bleavins MR, Zielinski D, Zandee JC.** 1998. Comparison of flow cytometric and manual bone marrow differentials. Cytometry **32:**9–17.
32. **Deshmane SL, Kremlev S, Amini S, Sawaya BE**. 2009. Monocyte chemoattractant protein 1 (MCP1): an overview. J Interferon Cytokine Res **29:**313–326.
33. **Deshpande S, Bosbach B, Yozgat Y, Park CY, Moore MA, Besmer P.** 2013. Kit receptor gain-of-function in hematopoiesis enhances stem cell self-renewal and promotes progenitor cell expansion. Stem Cells **31:**1683–1695.
34. **Ebmeyer J, Ebmeyer U, Pak K, Sudhoff H, Broide D, Ryan AF, Wasserman S.** 2010. Reconstitution of the mast cell population in W/Wv mice. Otol Neurotol **31:**42–47.
35. **Eckly A, Strassel C, Freund M, Cazenave JP, Lanza F, Gachet C, Leon C.** 2009. Abnormal megakaryocyte morphology and proplatelet formation in mice with megakaryocyte-restricted MYH9 inactivation. Blood **113:**3182–3189.
36. **Elmore SA.** 2006. Enhanced histopathology of the bone marrow. Toxicol Pathol **34:**666–686.
37. **Everds N.** 2007. Hematology of the laboratory mouse, p 135–163. In: Fox J, editor. The mouse in biomedical research. Waltham (MA): Academic Press.
38. **Fernandez GC, Lopez MF, Gomez SA, Ramos MV, Bentancor LV, Fernandez-Brando RJ, Landoni VI, Dran GI, Meiss R, Isturiz MA, Palermo MS.** 2006. Relevance of neutrophils in the murine model of

haemolytic uraemic syndrome: mechanisms involved in Shiga toxin type 2-induced neutrophilia. Clin Exp Immunol **146:**76–84.
39. **Fernández I, Peña A, Del Teso N, Pérez V, Rodríguez-Cuesta J.** 2010. Clinical biochemistry parameters in C57BL/6J mice after blood collection from the submandibular vein and retroorbital plexus. J Am Assoc Lab Anim Sci **49:**202–206.
40. **Festing MFW.** 2006. Design and statistical methods in studies using animal models of development. ILAR J **47:**5–14.
41. **Festing MFW, Altman DG**. 2002. Guidelines for the design and statistical analysis of experiments using laboratory animals. ILAR J **43:**244–258.
42. **Fitts DA.** 2011. Ethics and animal numbers: informal analysis, uncertain sample sizes, inefficient replications, and type I errors. J Am Assoc Lab Anim Sci **50:**445–453.
43. **Folgueras AR, de Lara FM, Pendas AM, Garabaya C, Rodriguez F, Astudillo A, Bernal T, Cabanillas R, Lopez-Otin C, Velasco G.** 2008. Membrane-bound serine protease matriptase 2 (Tmprss6) is an essential regulator of iron homeostasis. Blood **112:**2539–2545.
44. **Furuya Y, Inagaki A, Khan M, Mori K, Penninger JM, Nakamura M, Udagawa N, Aoki K, Ohya K, Uchida K, Yasuda H.** 2013. Stimulation of bone formation in cortical bone of mice treated with a receptor activator of nuclear factor-κB ligand (RANKL)-binding peptide that possesses osteoclastogenesis inhibitory activity. J Biol Chem **288:**5562–5571.
45. **Galli SJ.** 2000. Mast cells and basophils. Curr Opin Hematol **7:**32–39.
46. **Gervais F, Attia M.** 2005. Fibro-osseous proliferation in the sternums and femurs of female B6C3F1, C57BL, and CD1 mice: a comparative study. Dtsch Tierarztl Wochenschr **112:**323–326.
47. **Gibson JN, Jellen LC, Unger EL, Morahan G, Mehta M, Earley CJ, Allen RP, Lu L, Jones BC**. 2011. Genetic analysis of iron-deficiency effects on the mouse spleen. Mamm Genome **22:**556–562.
48. **Golde WT, Gollobin P, Rodriguez LL.** 2005. A rapid, simple, and humane method for submandibular bleeding of mice using a lancet. Lab Anim (NY) **34:**39–43.
49. **Golub R, Cumano A.** 2013. Embryonic hematopoiesis. Blood Cells Mol Dis **51:**226–231.
50. **Gray TE, Pratt MC, Cusick PK.** 1999. Determination of agreement between laboratory instruments. Contemp Top Lab Anim Sci **38:**56–59.
51. **Greinacher A.** 2011. Platelet activation by heparin. Blood **117:**4686–4687.
52. **Greth A, Lampkin S, Mayura-Guru P, Rodda F, Drysdale K, Roberts-Thomson M, McMorran BJ, Foote SJ,** Burgio GT**.** 2012. A novel ENU mutation in ankyrin 1 disrupts malaria parasite maturation in red blood cells of mice. PLoS ONE **7:**e38999.
53. **Grimaldi E, Scopacasa F.** 2000. Evaluation of the Abbott Cell-Dyn 4000 hematology analyzer. Am J Clin Pathol **113:**497–505.
54. **Guan H, Zhou Z, Cao Y, Duan X, Kleinerman ES.** 2009. VEGF165 promotes the osteolytic bone destruction of Ewing's sarcoma tumors by upregulating RANKL. Oncol Res **18:**117–125.
55. **Hao X, Fredrickson TN, Chattopadhyay SK, Han W, Qi CF, Wang Z, Ward JM, Hartley JW, Morse HC 3rd.** 2010. The histopathologic and molecular basis for the diagnosis of histiocytic sarcoma and histiocyte-associated lymphoma of mice. Vet Pathol **47:**434–445.
56. **Harvey JW.** 2001. Atlas of veterinary hematology. Philadelphia (PA): Saunders.
57. **Hasselbalch HC.** 2014. A role of NF-E2 in chronic inflammation and clonal evolution in essential thrombocythemia, polycythemia vera, and myelofibrosis? Leuk Res **38:**263–266.
58. **Hawley RG, Fong AZC, Burns BF, Hawley TS.** 1992. Transplantable myeloproliferative disease induced in mice by an interleukin 6 retrovirus. J Exp Med **176:**1149–1163.
59. **Hoff J.** 2000. Methods of blood collection in the mouse. Lab Anim (NY) **29:**47–53.
60. **Hol J, Wilhelmsen L, Haraldsen G.** 2010. The murine IL8 homologues KC, MIP2, and LIX are found in endothelial cytoplasmic granules but not in Weibel–Palade bodies. J Leukoc Biol **87:**501–508.
61. **Holmberg H, Kiersgaard MK, Mikkelsen LF, Tranholm M.** 2011. Impact of blood sampling technique on blood quality and animal welfare in haemophilic mice. Lab Anim **45:**114–120.
62. **Houwen B.** 2002. Blood film preparation and staining procedures. Clin Lab Med **22:**1–14.
63. **Ioannou YA, Zeidner KM, Gordon RE, Desnick RJ.** 2001. Fabry disease: preclinical studies demonstrate the effectiveness of α-galactosidase A replacement in enzyme-deficient mice. Am J Hum Genet **68:**14–25.
64. **Irons RD.** 1991. Blood and bone marrow, p 389–419. In: Haschek WM, Rousseaux CG, editors. Handbook of toxicologic pathology. San Diego (CA): Academic Press.
65. **Jackson CW, Steward SA, Chenaille PJ, Ashmun RA, McDonald TP.** 1990. An analysis of megakaryocytopoiesis in the C3H mouse: an animal model whose megakaryocytes have 32N as the modal DNA class. Blood **76:**690–696.
66. **Jain NC.** 1993. Comparative hematologic features of some avian and mammalian species, p 54–71. In: Jain NC, editor. Essentials of veterinary hematology. Philadelphia (PA): Lea and Febiger.
67. **Jay SM, Skokos EA, Zeng J, Knox K, Kyriakides TR.** 2010. Macrophage fusion leading to foreign body giant cell formation persists under phagocytic stimulation by microspheres in vitro and in vivo in mouse models. J Biomed Mater Res A **93:**189–199.
68. **Johns JL, Christopher MM.** 2012. Extramedullary hematopoiesis: a new look at the underlying stem cell niche, theories of development, and occurrence in animals. Vet Pathol **49:**508–523.
69. **Kang IG, Jung JH, Kim ST**. 2012. Asian sand dust enhances allergen-induced Th2 allergic inflammatory changes and mucin production in BALB/c mouse lungs. Allergy Asthma Immunol Res **4:**206–213. doi: 10.4168/aair.2012.4.4.206.
70. **Kauppi M, Hiltona AA, Metcalfa D, Nga AP, Hylanda CD, Collingea JE, Kilea BT, Hilton DJ, Alexandera WS.** 2012. Thrombocytopenia and erythrocytosis in mice with a mutation in the gene encoding the hemoglobin β minor chain. Proc Natl Acad Sci USA **109:**576–581.
71. **Kilkenny C, Browne WJ, Cuthill IC, Emerson M, Altman DG.** 2012. Improving bioscience research reporting: the ARRIVE guidelines for reporting animal research. PLoS ONE **20:**256–260.
72. **Kilkenny C, Parsons N, Kadyszewski E, Festing MFW, Cuthill IC, Fry D, Hutton J, Altman DG.** 2009. Survey of the quality of experimental design, statistical analysis, and reporting of research using animals. PLoS ONE **4:**e7824.
73. **Kirabo A, Park SO, Wamsley HL, Gali M, Baskin R, Reinhard MK, Zhao ZJ, Bisht KS, Keseru GM, Cogle CR, Sayeski PP.** 2012. The small-molecule inhibitor G6 significantly reduces bone marrow fibrosis and the mutant burden in a mouse model of Jak2-mediated myelofibrosis. Am J Pathol **181:**858–865.
74. **Kirby NA, Stepanek AM, Vernet A, Schmidt SM, Schultz CL, Parry NM, Niemi SM, Fox JG, Brown DE.** 2014. Urinary MCP1 and microalbumin increase prior to onset of azotemia in mice with polycystic kidney disease. Comp Med **64:**99–105.
75. **Knoll J.** 2000. Clinical automated hematology systems, p 3–11. In: Feldman BF, Zinkl JG, Jain NC, editors. Schalm's veterinary hematology. Hoboken (NJ): Wiley–Blackwell.
76. **Kogan SC.** 2002. Bethesda proposals for classification of nonlymphoid hematopoietic neoplasms in mice. Blood **100:**238–245.
77. **Kunder S, Calzada-Wack J, Holzlwimmer G, Muller J, Kloss C, Howat W, Schmidt J, Hofler H, Warren M, Quintanilla-Martinez L.** 2007. A comprehensive antibody panel for immunohistochemical analysis of formalin-fixed, paraffin-embedded hematopoietic neoplasms of mice: analysis of mouse-specific and human antibodies cross-reactive with murine tissue. Toxicol Pathol **35:**366–375.
78. **Kuter DJ, Bain B, Mufti G, Bagg A, Hasserjian RP.** 2007. Bone marrow fibrosis: pathophysiology and clinical significance of increased bone marrow stromal fibres. Br J Haematol **139:**351–362.
79. **Landoni VI, Chiarella P, Martire-Greco D, Schierloh P, van-Rooijen N, Rearte B, Palermo MS, Isturiz MA, Fernandez GC.** 2012. Tolerance to lipopolysaccharide promotes an enhanced neutrophil

extracellular traps formation leading to a more efficient bacterial clearance in mice. Clin Exp Immunol **168:**153–163.
80. **Lane SW, Sykes SM, Al-Shahrour F, Shterental S, Paktinat M, Lo Celso C, Jesneck JL, Ebert BL, Williams DA, Gilliland DG.** 2010. The *Apc^{min}* mouse has altered hematopoietic stem cell function and provides a model for MPD/MDS. Blood **115:**3489–3497.
81. **Lee J, Cacalano G, Camerato T, Toy K, Moore MW, Wood W.** 1995. Chemokine binding and activities mediated by the mouse IL8 receptor. J Immunol **155:**2158–2164.
82. **Lefkowitz JB.** 2008. Heparin-induced thrombocytopenia, p 287–294. In: Kottke-Marchant K, editor. An algorithmic approach to hemostasis testing. Northfield (IL): CAP Press.
83. **Léon C, Evert K, Dombrowski F, Pertuy F, Eckly A, Laeuffer P, Gachet C, Greinacher A.** 2012. Romiplostim administration shows reduced megakaryocyte response-capacity and increased myelofibrosis in a mouse model of MYH9-RD. Blood **119:**3333–3341.
84. **Levin J, Ebbe S.** 1994. Why are recently published platelet counts in normal mice so low. Blood **83:**3829–3831.
85. **Ley K, Miller YI, Hedrick CC.** 2011. Monocyte and macrophage dynamics during atherogenesis. Arterioscler Thromb Vasc Biol **31:**1506–1516.
86. **Lieschke GJ, Grail D, Hodgson G, Metcalf D, Stanley E, Cheers C, Fowler KJ, Basu S, Zhan YF, Dunn AR.** 1994. Mice lacking granulocyte colony-stimulating factor have chronic neutropenia, granulocyte, and macrophage progenitor cell deficiency, and impaired neutrophil mobilization. Blood **84:**1737–1746.
87. **Linden M, Ward JM, Cherian S.** 2011. Hematopoietic and lymphoid tissues, p 309–338. In: Trueting PM, Dintzis SM, editors. Comparative anatomy and histology: a mouse and human atlas. Amsterdam (the Netherlands): Elsevier.
88. **Liu G, Bi Y, Wang R, Shen B, Zhang Y, Yang H, Wang X, Liu H, Lu Y, Han F.** 2013. Kinase AKT1 negatively controls neutrophil recruitment and function in mice. J Immunol **191:**2680–2690.
89. **Liu J, Zhang J, Ginzburg Y, Li H, Xue F, De Franceschi L, Chasis JA, Mohandas N, An X.** 2013. Quantitative analysis of murine terminal erythroid differentiation in vivo movel method to study normal and disordered erythropoeisis. Blood **121:**e43–e49.
90. **Lundberg P, Skoda R.** 2011. Hematology testing in mice. Curr Prot Mouse Biol **1:**323–346.
91. **Lundorff JA, Kjelgaard-Hansen M**. 2006. Method comparison in the clinical laboratory. Vet Clin Pathol **35**:276–286.
92. **Magez S, Caljon G.** 2011. Mouse models for pathogenic African trypanosomes: unravelling the immunology of host–parasite–vector interactions. Parasite Immunol **33:**423–429.
93. **Marcos R, Santos M, Santos N, Malhao F, Ferreira F, Monteiro RA, Rocha E**. 2009. Use of destained cytology slides for the application of routine special stains. Vet Clin Pathol **38**:94–102.
94. **Mathers RA, Evans GO, Bleby J.** 2013. Platelet measurements in rat, dog, and mouse blood samples using the Sysmex XT2000iV. Comp Clin Pathol **22:**815–821.
95. **Maue RA, Burgess RW, Wang B, Wooley CM, Seburn KL, Vanier MT, Rogers MA, Chang CC, Chang TY, Harris BT, Graber DJ, Penatti CA, Porter DM, Szwergold BS, Henderson LP, Totenhagen JW, Trouard TP, Borbon IA, Erickson RP.** 2012. A novel mouse model of Niemann–Pick type C disease carrying a D1005G–Npc1 mutation comparable to commonly observed human mutations. Hum Mol Genet **21:**730–750.
96. **McCoy MW, Moreland SM, Detweiler CS.** 2012. Hemophagocytic macrophages in murine typhoid fever have an antiinflammatory phenotype. Infect Immun **80:**3642–3649.
97. **McDonald TP, Clift RE, Cottrell MB.** 1992. Large chronic doses of erythropoietin cause thrombocytopenia in mice. Blood **80:**352–358.
98. **Min B, Prout M, Hu-Li J, Zhu J, Jankovic D, Morgan ES, Urban JF Jr, Dvorak AM, Finkelman FD, LeGros G, Paul WE.** 2004. Basophils produce IL4 and accumulate in tissues after infection with a Th2-inducing parasite. J Exp Med **200:**507–517.
99. **Monack DM, Bouley DM, Falkow S.** 2004. *Salmonella typhimurium* persists within macrophages in the mesenteric lymph nodes of chronically infected *Nramp1$^{+/+}$* mice and can be reactivated by IFNγ neutralization. J Exp Med **199:**231–241.
100. **Moore D.** 2000. Hematology of the mouse (*Mus musculus*), p 1219–1224. In: Feldman BF, Zinkl JG, Jain NC, editors. Schalm's veterinary hematology. Hoboken (NJ): Wiley–Blackwell.
101. **Morohashi K-i, Tsuboi-Asai H, Matsushita S, Suda M, Nakashima M, Sasano H, Hataba Y, Li C-L, Fukata J, Irie J, Watanabe T, Nagura H, Li E.** 1999. Structural and functional abnormalities in the spleen of *anmFtz–F1* gene-disrupted mouse. Blood **93:**1586–1594.
102. **Mullally A, Poveromo L, Schneider RK, Al-Shahrour F, Lane SW, Ebert BL.** 2012. Distinct roles for long-term hematopoietic stem cells and erythroid precursor cells in a murine model of Jak2V617F-mediated polycythemia vera. Blood **120:**166–172.
103. **Murone M, Carpenter DA, de Sauvage FJ.** 1998. Hematopoietic deficiencies in c-mpl and TPO knockout mice. Stem Cells **16:**1–6.
104. **Nagahisa H, Nagata Y, Ohnuki T, Osada M, Nagasawa T, Abe T, Todokoro K.** 1996. Bone marrow stromal cells produce thrombopoietin and stimulate megakaryocyte growth and maturation but suppress proplatelet formation. Blood **87:**1309–1316.
105. **Nagarajan P, Shailendra A, Venkatesan R, Kumar MJM, Majumdar SS, Juyal RC.** 2012. Sex- and strain-related differences in the peripheral blood cell values of mutant mouse strains. Comp Clin Pathol **21:**1577–1585.
106. **Narahara S, Matsushima H, Sakai E, Fukuma Y, Nishishita K, Okamoto K, Tsukuba T.** 2012. Genetic backgrounds and redox conditions influence morphological characteristics and cell differentiation of osteoclasts in mice. Cell Tissue Res **348:**81–94.
107. **Naveiras O, Nardi V, Wenzel PL, Hauschka PV, Fahey F, Daley GQ.** 2009. Bone-marrow adipocytes as negative regulators of the haematopoietic microenvironment. Nature **460:**259–263.
108. **Nganga VK, Palmer VL, Naushad H, Kassmeier MD, Anderson DK, Perry GA, Schabla NM, Swanson PC.** 2013. Accelerated progression of chronic lymphocytic leukemia in Eμ-TCL1 mice expressing catalytically inactive RAG1. Blood **121:**3855–3866.
109. **NIH Reporter.** 2014. [Internet]. Research Portfolio Online Reporting Tools. [Cited 10 July 2014]. Available at: http://projectreporter.nih.gov/reporter.cfm.
110. **Oldenborg PA.** 2002. Lethal autoimmune hemolytic anemia in CD47-deficient nonobese diabetic (NOD) mice. Blood **99:**3500–3504.
111. **Onah DN, Wakelin D.** 2000. Murine model study of the practical implication of trypanosome-induced immunosuppression in vaccine-based disease control programmes. Vet Immunol Immunopathol **74:**271–284.
112. **Ooi YY, Rahmat Z, Jose S, Ramasamy R, Vidyadaran S**. 2013. Immunophenotype and differentiation capacity of bone marrow-derived mesenchymal stem cells from CBA/Ca, ICR, and Balb/c mice. World J Stem Cells **5:**34–42.
113. **Papasouliotis K, Cue S, Crawford E, Pinches M, Dumont M, Burley K**. 2006. Comparison of white blood cell differential percentages determined by the inhouse LaserCyte hematology analyzer and a manual method. Vet Clin Pathol **35:**295–302.
114. **Percy DH, Barthold SW.** 2007. Mouse, p. 3–124. In: Percy DH, Barthold SW, editors. Pathology of laboratory rodents and rabbits. Ames (IA): Blackwell Publishing.
115. **Perel P, Roberts I, Sena E, Wheble P, Briscoe C, Sandercock P, Macleod M, Mignini LE, Jayaram P, Khan KS.** 2007. Comparison of treatment effects between animal experiments and clinical trials: systematic review. Br Med J **334:**197.
116. **Peters LL, Cheever EM, Ellis HR, Magnani PA, Svenson KL, Von Smith R, Bogue MA.** 2002. Large-scale, high-throughput screening for coagulation and hematologic phenotypes in mice. Physiol Genomics **11:**185–193.
117. **Phan VT, Wu X, Cheng JH, Sheng RX, Chung AS, Zhuang G, Tran C, Song Q, Kowanetz M, Sambrone A, Tan M, Meng YG, Jackson EL, Peale FV, Junttila MR, Ferrara N.** 2013. Oncogenic RAS pathway activation promotes resistance to antiVEGF therapy through G-CSF-induced neutrophil recruitment. Proc Natl Acad Sci USA **110:**6079–6084.

118. **Pipitone S, Pavesi F, Testa B, Bardi M, Perri GB, Gennari D, Lippi G**. 2012. Evaluation of automated nucleated red blood cells counting on Sysmex XE5000 and Siemens Advia 2120. Clin Chem Lab Med **50:**1857–1859.
119. **Provencher Bolliger A, Everds NE, Zimmerman KL, Moore DM, Smith SA, Barnhart KF.** 2010. Hematology of laboratory animals, p 852–887. In: Weiss D, Wardrop J, Schalm OW, editors. Schalm's veterinary hematology. Hoboken (NJ): Wiley–Blackwell.
120. PubMed. 2014. [Internet]. PubMed - Official Site. [Cited 10 July 2014]. Available at: http://www.ncbi.nlm.nih.gov/pubmed
121. **Putz G, Rosner A, Nuesslein I, Schmitz N, Buchholz F.** 2006. AML1 deletion in adult mice causes splenomegaly and lymphomas. Oncogene **25:**929–939.
122. **Qian S, Fu F, Li W, Chen Q, Sauvage FJ.** 1998. Primary role of the liver in thrombopoietin production shown by tissue-specific knockout. Blood **92:**2189–2191.
123. **Raabe BM, Artwohl JE, Purcell JE, Lovaglio J, Fortman JD.** 2011. Effects of weekly blood collection in C57BL/6 mice. J Am Assoc Lab Anim Sci **50:**680–685.
124. **Raben N, Wong A, Ralston E, Myerowitz R.** 2012. Autophagy and mitochondria in Pompe disease: nothing is so new as what has long been forgotten. Am J Med Genet C Semin Med Genet **160C:**13–21.
125. **Ramsey H, Zhang Q, Brown DE, Steensma DP, Lin CP, Wu MX.** 2014. Stress-induced hematopoietic failure in the absence of immediate early response gene X1. Haematologica **99:**282–291.
126. **Raskin RE.** 2010. Cytochemical staining, p 1141–1156. In: Weiss DJ, Wardrop KJ, editors. Schalm's veterinary hematology. Hoboken (NJ): Wiley–Blackwell.
127. **Reagan WJ, Irizarry-Rovira A, Poitout-Belissent F, Bolliger AP, Ramaiah SK, Travlos G, Walker D, Bounous D, Walter G**. 2011. Best practices for evaluation of bone marrow in nonclinical toxicity studies. Vet Clin Pathol **40:**119–134.
128. **Rehg JE, Bush D, Ward JM.** 2012. The utility of immunohistochemistry for the identification of hematopoietic and lymphoid cells in normal tissues and interpretation of proliferative and inflammatory lesions of mice and rats. Toxicol Pathol **40:**345–374.
129. **Rittinghausen S, Kohler M, Kamino K, Dasenbrock C, Mohr U.** 1997. Spontaneous myelofibrosis in castrated and ovariectomized NMRI mice. Exp Toxicol Pathol **49:**351–353.
130. **Russell ES, Bernstein SE.** 1966. Blood and blood formation, p 351–372. In: Green EL, editor. Biology of the laboratory mouse. New York (NY): McGraw Hill.
131. **Russell WMS, Burch RL.** 1959. The principles of humane experimental technique. London (United Kingdom): Methuen.
132. **Samuels A, Perry MJ, Tobias JH.** 1999. High-dose estrogen induces de novo medullary bone formation in female mice. J Bone Miner Res **14:**178–186.
133. **Schlegel R, MacGregor JT.** 1983. A rapid screen for cumulative chromosomal damage in mice, accumulation of circulating micronucleated erythrocytes. Mutat Res **113:**481–487.
134. **Schmitt A, Guichard J, Masse J-M, Debili N, Cramer EM.** 2001. Of mice and men: comparison of the ultrastructure of megakaryocytes and platelets. Exp Hematol **29:**1295–1302.
135. **Schwab CL, Fan R, Zheng Q, Myers LP, Hebert P, Pruett SB**. 2005. Modeling and predicting stress-induced immunosuppression in mice using blood parameters. Toxicol Sci **83:**101–113.
136. **Seder RA, Paul WE, Dvorak AM, Sharkis SJ, Kagey-Sobotka A, Niv Y, Finkelman FD, Barbier SA, Galli SJ, Plaut M.** 1991. Mouse splenic and bone marrow cell populations that express high-affinity FcE receptors and produce interleukin 4 are highly enriched in basophils. Proc Natl Acad Sci USA **88:**2835–2839.
137. **Sellers RS, Clifford CB, Treuting PM, Brayton C.** 2012. Immunological variation between inbred laboratory mouse strains: points to consider in phenotyping genetically immunomodified mice. Vet Pathol **49:**32–43.
138. **Senchenkova EY, Komoto S, Russell J, Almeida-Paula LD, Yan LS, Zhang S, Granger DN.** 2013. Interleukin 6 mediates the platelet abnormalities and thrombogenesis associated with experimental colitis. Am J Pathol **183:**173–181.
139. **Senyuk V, Rinaldi CR, Li D, Cattaneo F, Stojanovic A, Pane F, Du X, Mahmud N, Dickstein J, Nucifora G.** 2009. Consistent upregulation of Stat3 independently of Jak2 mutations in a new murine model of essential thrombocythemia. Cancer Res **69:**262–271.
140. **Shetty VT.** 2001. Pseudo Pelger–Huet anomaly in myelodysplastic syndrome: hyposegmented or apoptotic neutrophil? Blood **98:**1273–1275.
141. **Shi C, Pamer EG.** 2011. Monocyte recruitment during infection and inflammation. Nat Rev Immunol **11:**762–774.
142. **Shirasaki Y, Ito Y, Kikuchi M, Imamura Y, Hayashi T.** 2012. Validation studies on blood collection from the jugular vein of conscious mice. J Am Assoc Lab Anim Sci **51:**345–351.
143. **Shultz LD, Lyons BL, Burzenski LM, Gott B, Samuels R, Schweitzer PA, Dreger C, Herrmann H, Kalscheuer V, Olins AL, Olins DE, Sperling K, Hoffmann K.** 2003. Mutations at the mouse ichthyosis locus are within the lamin B receptor gene—a single gene model for human Pelger–Huët anomaly. Hum Mol Genet **12:**61–69.
144. **Smith GS.** 2000. Neutrophils, p. 281–296. In: Feldman BF, Zinkl JG, Jain NC, editors. Schalm's veterinary hematology. Hoboken (NJ): Wiley–Blackwell.
145. **Snider CL, Dick EJ Jr, McGlasson DL, Robbins MC, Sholund RL, Bommineni YR, Hubbard GB.** 2009. Evaluation of 4 hematology and a chemistry portable benchtop analyzers using nonhuman primate blood. J Med Primatol **38:**390–396.
146. **Socolovsky M, Nam H-s, Fleming MD, Haase VH, Brugnara C, Lodish HF.** 2001. Ineffective erythropoiesis in *Stat5a*$^{-/-}$*5b*$^{-/-}$ mice due to decreased survival of early erythroblasts. Blood **98:**3261–3273.
147. **Staropoli JF, Haliw L, Biswas S, Garrett L, Hölter SM, Becker L, Skosyrski S, Da Silva-Buttkus P, Calzada-Wack J, Neff F, Rathkolb B, Rozman J, Schrewe A, Adler T, Puk O, Sun M, Favor J, Racz I, Bekeredjian R, Busch DH, Graw J, Klingenspor M, Klopstock T, Wolf E, Wurst W, Zimmer A, Lopez E, Harati H, Hill E, Krause DS, Guide J, Dragileva E, Gale E, Wheeler V, Boustany RM, Brown DE, Breton S, Ruether K, Gailus-Durner V, Fuchs H, de Angelis MH, Cotman S.** 2012. Large-scale phenotyping of an accurate genetic mouse model of JNCL identifies novel early pathology outside the central nervous system. PLoS ONE **7:**e38310.
148. Stockham SL**.** 2008. Leukocytes, p 53–106. In: Stockham SL, Scott MA, editors. Fundamentals of veterinary clinical pathology. Ames (IA): Blackwell Publishing.
149. **Stoffel R, Wiestner A, Skoda R.** 1996. Thrombopoietin in thrombocytopenic mice—evidence against regulation at the mRNA level and for a direct regulatory role of platelets. Blood **87:**567–573.
150. **Strassel C, Eckly A, Leon C, Petitjean C, Freund M, Cazenave JP, Gachet C, Lanza F.** 2009. Intrinsic impaired proplatelet formation and microtubule coil assembly of megakaryocytes in a mouse model of Bernard–Soulier syndrome. Haematologica **94:**800–810.
151. **Sudo K, Ema H, Morita Y, Nakauchi H.** 2000. Age-associated characteristics of murine hematopoietic stem cells. J Exp Med **192:**1273–1280.
152. **Sun CC, Vaja V, Babitt JL, Lin HY.** 2012. Targeting the hepcidin–ferroportin axis to develop new treatment strategies for anemia of chronic disease and anemia of inflammation. Am J Hematol **87:**392–400.
153. **Suttie AW.** 2006. Histopathology of the spleen. Toxicol Pathol **34:**466–503.
154. **Takaku T, Malide D, Chen J, Calado RT, Kajigaya S, Young NS.** 2010. Hematopoiesis in 3 dimensions: human and murine bone marrow architecture visualized by confocal microscopy. Blood **116:**e41–e55.
155. **Tomlinson L, Boone LI, Ramaiah L, Penraat KA, von Beust BR, Ameri M, Poitout-Belissent FM, Weingand K, Workman HC, Aulbach AD, Meyer DJ, Brown DE, Macneill AL, Bolliger AP, Bounous DI**. 2013. Best practices for veterinary toxicologic clinical pathology, with emphasis on the pharmaceutical and biotechnology industries. Vet Clin Pathol **42**:252–269. .

156. **Travlos GS.** 2006. Normal structure, function, and histology of the bone marrow. Toxicol Pathol **34:**548–565.
157. **Treuting PM, Clifford CB, Sellers RS, Brayton CF.** 2012. Of mice and microflora: considerations for genetically engineered mice. Vet Pathol **49:**44–63.
158. **Tvedten H**. 1993. Advanced hematology analyzers: interpretation of results. Vet Clin Pathol **22:**72–80.
159. **Tvedten H**. 2009. Atypical mitoses. Vet Clin Pathol **38:**418–420.
160. **van Furth R.** 1989. Origin and turnover of monocytes and macrophages. Curr Top Pathol **79:**125–150.
161. **Vap LM, Harr KE, Arnold JE, Freeman KP, Getzy K, Lester S, Friedrichs KR**. 2012. ASVCP quality assurance guidelines: control of preanalytical and analytical factors for hematology for mammalian and nonmammalian species, hemostasis, and crossmatching in veterinary laboratories. Vet Clin Pathol **41:**8–17.
162. **Walton RM**. 2012. Subject-based reference values: biological variation, individuality, and reference change values. Vet Clin Pathol **41**:175–181.
163. **Wancket LM, Devor-Henneman D, Ward JM.** 2008. Fibroosseous (FOL) and degenerative joint lesions in female outbred NIH Black Swiss mice. Toxicol Pathol **36:**362–365.
164. **Ward JM, Rehg JE, Morse HC 3rd.** 2012. Differentiation of rodent immune and hematopoietic system reactive lesions from neoplasias. Toxicol Pathol **40:**425–434.
165. **Watanabe S, Terashima K, Ohta S, Horibata S, Yajima M, Shiozawa Y, Dewan MZ, Yu Z, Ito M, Morio T, Shimizu N, Honda M, Yamamoto N.** 2007. Hematopoietic stem cell-engrafted NOD/SCID/IL2Rγ-null mice develop human lymphoid systems and induce long-lasting HIV1 infection with specific humoral immune responses. Blood **109:**212–218.
166. **Webb JL, Latimer KS.** 2011. Leukocytes, p 45–82. In: Latimer KS, editor. Veterinary laboratory medicine: clinical pathology. Hoboken (NJ): Wiley–Blackwell.
167. **Weih F, Carrasco D, Durham SK, Barton DS, Rizzo CA, Ryseck R-P, Lira SA, Bravo R.** 1995. Multiorgan inflammation and hematopoietic abnormalities in mice with a targeted disruption of RelB, a member of the NFκB–Rel family. Cell **80:**331–340.
168. **Weiser G.** 2012. Laboratory technology for veterinary medicine, p 3–33. In: Thrall MA, Weiser G, Allison RW, editors. Veterinary hematology and clinical chemistry. Hoboken (NJ): John Wiley and Sons.
169. **Weiser G.** 2012. Neutrophil production, trafficking, and kinetics, p. 123–126. In: Thrall MA, Weiser G, Allison RW, editors. Veterinary hematology and clinical chemistry. Hoboken (NJ): John Wiley and Sons.
170. **Weiss DJ, Wilkerson MJ.** 2010. Flow cytometry, p 1047–1081. In: Weiss DJ, Wardrop KJ, editors. Schalm's veterinary hematology. Hoboken (NJ): Wiley–Blackwell.
171. **Wickstrom SL, Oberg L, Karre K, Johansson MH.** 2014. A genetic defect in mice that impairs missing self recognition despite evidence for normal maturation and MHC class I-dependent education of NK cells. J Immunol **192:**1577–1586.
172. **Yaccoby S, Barlogie B, Epstein J.** 1998. Primary myeloma cells growing in SCID–hu mice: a model for studying the biology and treatment of myeloma and its manifestations. Blood **92:**2908–2913.
173. **Yamada Y, Cancelas JA, Rothenberg ME.** 2009. Murine model of hypereosinophilic syndromes/chronic eosinophilic leukemia. Int Arch Allergy Immunol **149 Suppl 1:**102–107.
174. **Yildirim E, Kirby J, Brown D, Mercier F, Sadreyev R, Scadden D, Lee J.** 2013. *Xist* RNA is a potent suppressor of hematologic cancer in mice. Cell **152:**727–742.
175. **Yin L, Unger EL, Jellen LC, Earley CJ, Allen RP, Tomaszewicz A, Fleet JC, Jones BC.** 2012. Systems genetic analysis of multivariate response to iron deficiency in mice. Am J Physiol Regul Integr Comp Physiol **302:**R1282–R1296.
176. **Zeiss CJ, Ward JM, Allore HG.** 2012. Designing phenotyping studies for genetically engineered mice. Vet Pathol **49:**24–31.
177. **Zhang B, Kracker S, Yasuda T, Casola S, Vanneman M, Homig-Holzel C, Wang Z, Derudder E, Li S, Chakraborty T, Cotter SE, Koyama S, Currie T, Freeman GJ, Kutok JL, Rodig SJ, Dranoff G, Rajewsky K.** 2012. Immune surveillance and therapy of lymphomas driven by Epstein–Barr virus protein LMP1 in a mouse model. Cell **148:**739–751.
178. **Zhu M, Lovell KL, Patterson JS, Saunders TL, Hughes ED, Friderici KH.** 2005. β-mannosidosis mice: a model for the human lysosomal storage disease. Hum Mol Genet **15:**493–500.